

Title: Twin support vector quantile regression

Author names and affiliations:

Yafen Ye

School of Economics, Zhejiang University of Technology, Hangzhou, 310023,
P.R.China

Institute for Industrial System Modernization, Zhejiang University of Tech-
nology, Hangzhou, 310023, P.R.China
yafenye@163.com

Zhihu Xu

School of Economics, Zhejiang University of Technology, Hangzhou, 310023,
P.R.China

dianxianquan@126.com

Jinhua Zhang

School of Economics, Zhejiang University of Technology, Hangzhou, 310023,
P.R.China

celliazjh@zjut.edu.cn

Weijie Chen

School of Economics, Zhejiang University of Technology, Hangzhou, 310023,
P.R.China

Zhijiang College, Zhejiang University of Technology, Hangzhou, 310023, P.R.China
wjcp2008@126.com

Yuanhai Shao

Management School, Hainan University, Haikou, 570228, P. R. China
shaoyuanhai21@163.com

Corresponding Author:

Yuanhai Shao

Management School, Hainan University, Haikou, 570228, P. R. China
shaoyuanhai21@163.com

Twin support vector quantile regression

Yafen Ye^{a,b}, Zhihu Xu^a, Jinhua Zhang^a, Weijie Chen^{a,c}, Yuanhai Shao^{d,*}

^a*School of Economics, Zhejiang University of Technology, Hangzhou, 310023, P.R.China*

^b*Institute for Industrial System Modernization, Zhejiang University of Technology, Hangzhou, 310023, P.R.China*

^c*Zhijiang College, Zhejiang University of Technology, Hangzhou, 310023, P.R.China*

^d*Management School, Hainan University, Haikou, 570228, P. R. China*

Abstract

We propose a twin support vector quantile regression (TSVQR) to capture the heterogeneous and asymmetric information in modern data. Using a quantile parameter, TSVQR effectively depicts the heterogeneous distribution information with respect to all portions of data points. Correspondingly, TSVQR constructs two smaller sized quadratic programming problems (QPPs) to generate two nonparallel planes to measure the distributional asymmetry between the lower and upper bounds at each quantile level. The QPPs in TSVQR are smaller and easier to solve than those in previous quantile regression methods. Moreover, the dual coordinate descent algorithm for TSVQR also accelerates the training speed. Experimental results on six artificial data sets, five benchmark data sets, two large scale data sets, two time-series data sets, and two imbalanced data sets indicate that the TSVQR outperforms previous quantile regression methods in terms of the effectiveness of completely capturing the heterogeneous and asymmetric information and the efficiency of the learning process.

Keywords: Twin support vector regression, quantile regression, heterogeneity, asymmetry.

1. Introduction

Heterogeneity, as one of the major statistical features of modern data (Wang, 2017), has commonly emerged in diverse fields, such as economics

*Corresponding author: shaoyuanhai21@163.com

(Tran et al., 2019; Ye et al., 2022), finance (Dirick et al., 2021), environment (Yang et al., 2021), genetics (Miller et al., 2021), and medicine (Khan et al., 2021). Moreover, in some real-world applications, the heterogeneity problem has always been accompanied by an asymmetry problem (Kolasa, 2009; Kundaje et al., 2012; Baigh et al., 2021). In the medicine field, for instance, the impact of temperature on COVID-19 in Indian states is heterogeneous and asymmetric (Irfan et al., 2022).

Regression technology, as an effective data analysis tool, presents challenges in dealing with the problem of heterogeneity and asymmetry. Ordinary least squares (OLS) regression (Dempster et al., 1977) is one of the commonly used methods for the estimation of the optimal regression function because its estimators have the smallest variance among the class of linear unbiased estimators. Unfortunately, least squares regression is a conditional mean model that only reflects the mean of the conditional distribution of data points. Least squares regression is not suitable for the problem of distributional heterogeneity. To deal with the distributional heterogeneity problem, Koenker and Bassett (1978) proposed quantile regression (QR) which uses a quantile parameter to compute several different regression curves corresponding to various percentage points of the distributions. As the quantile parameter increases, the estimated lines move up through the data, retaining in most cases a slope reasonably close to that of the family of true conditional quantile functions. QR offers a comprehensive strategy for obtaining a more complete picture of the data points, and has been an effective model to address the problem of distributional heterogeneity. Therefore, numerous extensions and variants of QR have been proposed (Wang et al., 2023a).

In the field of machine learning, support vector regression (SVR) (Drucker et al., 1997; Burges, 1998; Wu & Wang, 2022; Wang et al., 2023b) in the framework of statistical learning theory is an effective regression model. SVR adopts the L_2 -norm regularization term for the estimation of the optimal regression function, effectively overcoming the overfitting problem. Takeuchi et al. (2006) brought the technique of QR into the SVR framework, and proposed non-parametric quantile regression (NPQR). Subsequently, support vector quantile regression (SVQR) (Li et al., 2007; Park & Kim, 2011), support vector machine with generalized quantile loss (RQSVR) (Yang & Dong, 2019), ε -insensitive support vector quantile regression (ε -SVQR) (Anand et al., 2020), and online support vector quantile regression (Online-SVQR) (Ye et al., 2021) were proposed. These models follow the spirit of QR and use the quantile parameter to measure the various percentage points of the distributions. How-

ever, all of them use two parallel hyperplanes to find the decision function, which may lose the asymmetric information for all data points.

Twin support vector regression (TSVR) (Peng, 2010; Gupta & Gupta, 2019; Gupta & Gupta, 2021c; Shi & Chen, 2023; Gu et al., 2023) aims to generate two nonparallel functions such that each function determines the ε -insensitive lower or upper bounds of the unknown regressor, which can reflect the asymmetric information in data points. Shao et al. (2013) added a regularization term into TSVR, and proposed ε -twin support vector regression (ε -TSVR). ε -TSVR yields the dual problems to be stable positive definite quadratic programming problems, and improves the performance of regression. To improve the generalization performance, an asymmetric ν -twin support vector regression with pinball loss (Asy- ν -TSVR) (Xu et al., 2018) was proposed. Subsequently, an asymmetric Lagrangian ν -twin with pinball loss (URALTSVR) (Gupta & Gupta, 2021a) was proposed to control the fitting error inside the asymmetric tube. Although two unparallel hyperplanes in the framework of TSVR effectively reflect the asymmetric information, the use of this approach may lead to the loss of the unobserved heterogeneous information for all data points.

To capture the unobservable heterogeneous and asymmetric information in data points simultaneously, we bring the spirit of QR into ε -TSVR, and then propose a twin support vector quantile regression (TSVQR). On the one hand, TSVQR uses a quantile parameter to estimate the relationships between variables for all portions of a probability distribution. TSVQR provides multiple trends of the distribution, capturing the disparity in trends caused by heterogeneity. On the other hand, TSVQR aims to generate two nonparallel functions at each quantile level such that each function determines the ε -insensitive lower or upper bounds of the unknown regressor, which effectively captures the asymmetric information for each quantile level of the distribution. Therefore, TSVQR has the ability to capture the heterogeneous and asymmetric information in all data points simultaneously. Moreover, TSVQR solves two smaller-sized quadratic programming problems (QPPs), and each QPP has only one group of constraints for all data points. The strategy of solving two smaller-sized QPPs makes TSVQR work quickly. In addition, dual coordinate descent algorithm is adopted to solve the QPPs, which also accelerates the learning speed. The experimental results of six artificial data sets and five benchmark data sets demonstrate that TSVQR is much faster than SVQR, ε -SVQR, Online-SVQR, and a group penalized pseudo quantile regression (GPQR) (Ouhourane et al., 2022). Furthermore,

TSVQR captures the heterogeneous and asymmetric information at each quantile level and offers a more complete view of the statistical landscape and the relationships among variables than SVQR, ε -SVQR, Online-SVQR, and GPQR. To sum up, the main contributions of this paper are summarized as follows:

(i) TSVQR uses the quantile parameter to minimize an asymmetric version of errors, which yields a family of regression curves corresponding to different quantile levels and thus captures the heterogeneous information in data points.

(ii) TSVQR generates two nonparallel planes to measure the asymmetric distribution between the lower and upper bounds of each given quantile level, thus effectively capturing the asymmetric information at each given quantile level.

(iii) TSVQR solves two smaller quadratic programming problems and its each QPP has one group of constraints, which reduces the computational complexity. Moreover, the dual coordinate descent algorithm is adopted to solve its each QPP, leading to an accelerated learning speed.

(iv) The numerical experimental results and the statistical test results show that TSVQR outperforms SVQR, ε -SVQR, GPQR, and Online-SVQR in terms of the effectiveness of completely capturing the heterogeneous and asymmetric information. As the efficiency of the learning process, the training speed of TSVQR and URALTSVR is significantly faster than SVQR, ε -SVQR, GPQR, and Online-SVQR.

The rest of this paper is organized as follows. Section 2 briefly introduces related works. In Section 3, we propose TSVQR in detail. Section 4 describes the artificial and benchmark data set experiments, and section 5 shows the application of TSVQR to big data sets. Section 6 concludes this paper.

2. Background

We briefly review SVR, SVQR, TSVR, and ε -TSVR that are closely related to twin support vector quantile regression (TSVQR). For simplicity, it is only concerned with the linear version. Table 1 lists the corresponding notations of these methods.

2.1. Support vector regression

The optimal regression function of SVR is constructed as follows

$$f(x) = \mathbf{w}^T x + b, \tag{1}$$

Table 1: List of notations.

Notation	Description	Notation	Description
\mathbf{A}	input	\mathbf{Y}	the response column vector
(\mathbf{A}_i, y_i)	the i -th training sample	(\mathbf{A}, \mathbf{Y})	the training set
ξ and ξ^*	slack variables	\mathbf{e}	a vector of ones
\mathbf{w}	the coefficients of the decision function	b	an intercept
\mathbf{w}_1	the coefficients of lower-bound function	\mathbf{w}_2	the coefficients of up-bound function
b_1	an intercept of lower-bound function	b_2	an intercept of up-bound function
τ	a quantile parameter	\mathbf{K}	kernel matrix
C, C_1, C_2	parameters	$\varepsilon, \varepsilon_1, \varepsilon_2$	insensitive parameters

where $\mathbf{w} \in R^n$ denotes the coefficients of the decision function, and $b \in R$ is an intercept.

In standard SVR (Drucker et al., 1997), parameters \mathbf{w} and b in the regression function (1) are estimated by solving the following optimization problem

$$\begin{aligned}
& \min_{\mathbf{w}, b, \xi, \xi^*} \frac{1}{2} \|\mathbf{w}\|^2 + C \mathbf{e}^\top (\xi + \xi^*) \\
& \text{s.t. } \mathbf{Y} - (\mathbf{A}\mathbf{w} + b\mathbf{e}) \leq \varepsilon \mathbf{e} + \xi, \quad \xi \geq \mathbf{0}, \\
& \quad (\mathbf{A}\mathbf{w} + b\mathbf{e}) - \mathbf{Y} \leq \varepsilon \mathbf{e} + \xi^*, \quad \xi^* \geq \mathbf{0},
\end{aligned} \tag{2}$$

where $\|\cdot\|^2$ represents the L_2 -norm, $C > 0$ is a parameter determining the trade-off between the regularization term and empirical risk, ξ and ξ^* are slack variables, \mathbf{e} is a vector of ones of appropriate dimensions, and $\varepsilon > 0$ is an insensitive parameter. Note that, the constraints in (2) are adopted to generate two parallel planes that locate more training samples locate in the flat region. Therefore, SVR is not suitable for solving the existence of asymmetry since two parallel planes cannot reflect the asymmetric information of the training samples.

2.2. Support vector quantile regression

In standard SVQR, \mathbf{w} and b in the regression function (1) are estimated by minimizing

$$\begin{aligned}
& \min_{\mathbf{w}, b} \frac{1}{2} \|\mathbf{w}\|^2 + C(1 - \tau) \mathbf{e}^\top \xi + C\tau \mathbf{e}^\top \xi^* \\
& \text{s.t. } \mathbf{Y} - (\mathbf{A}\mathbf{w} + b\mathbf{e} + \xi) \leq \xi, \quad \xi \geq \mathbf{0}, \\
& \quad (\mathbf{A}\mathbf{w} + b\mathbf{e} + \xi^*) - \mathbf{Y} \leq \xi^*, \quad \xi^* \geq \mathbf{0},
\end{aligned} \tag{3}$$

where $\|\cdot\|^2$ represents the L_2 -norm, $C > 0$ is a parameter determining the trade-off between the regularization term and empirical risk, ξ and ξ^* are slack variables, \mathbf{e} is a vector of ones of appropriate dimensions, and τ ($0 < \tau < 1$) is a quantile parameter. SVQR minimizes the pinball loss function along with L_2 -norm regularization term for the estimation of the optimal regression function. The pinball loss function in SVQR captures the information of training samples at different quantiles. Thus, SVQR is suitable for solving the heterogeneous problem. The basic idea of SVQR is to find the final decision function by maximizing the margin between two parallel hyperplanes. However, using two parallel hyperplanes to find the decision function is not suitable for the existence of asymmetric information in the training data set.

2.3. Twin support vector regression

Different from SVR and SVQR, linear TSVR (Peng, 2010) seeks a pair of lower-bound and upper-bound functions

$$f_1(x) = \mathbf{w}_1^T x + b_1,$$

and

$$f_2(x) = \mathbf{w}_2^T x + b_2,$$

where $\mathbf{w}_1 \in R^n$, $\mathbf{w}_2 \in R^n$, $b_1 \in R$, and $b_2 \in R$.

The linear TSVR can be formulated as the following minimization problems

$$\begin{aligned} \min_{\mathbf{w}_1, b_1, \xi} & \frac{1}{2} [\mathbf{Y} - \mathbf{e}\varepsilon_1 - (\mathbf{A}\mathbf{w}_1 + b_1\mathbf{e})]^T [\mathbf{Y} - \mathbf{e}\varepsilon_1 - (\mathbf{A}\mathbf{w}_1 + b_1\mathbf{e})] + C_1 \mathbf{e}^T \xi \\ \text{s.t.} & \mathbf{Y} - (\mathbf{A}\mathbf{w}_1 + b_1\mathbf{e}) \geq \varepsilon_1 \mathbf{e} - \xi, \xi \geq \mathbf{0}, \end{aligned}$$

and

$$\begin{aligned} \min_{\mathbf{w}_2, b_2, \xi^*} & \frac{1}{2} [\mathbf{Y} + \mathbf{e}\varepsilon_2 - (\mathbf{A}\mathbf{w}_2 + b_2\mathbf{e})]^T [\mathbf{Y} + \mathbf{e}\varepsilon_2 - (\mathbf{A}\mathbf{w}_2 + b_2\mathbf{e})] + C_2 \mathbf{e}^T \xi^* \\ \text{s.t.} & (\mathbf{A}\mathbf{w}_2 + b_2\mathbf{e}) - \mathbf{Y} \geq \varepsilon_2 \mathbf{e} - \xi^*, \xi^* \geq \mathbf{0}, \end{aligned}$$

where $C_1 > 0$, $C_2 > 0$, $\varepsilon_1 > 0$ and $\varepsilon_2 > 0$ are parameters, and ξ and ξ^* are slack variables.

Shao et al. (2013) brought the structural risk minimization principle into TSVR, and proposed ε -twin support vector regression (ε -TSVR) as follows:

$$\begin{aligned} \min_{\mathbf{w}_1, b_1, \xi} & \frac{1}{2}C_3(\|\mathbf{w}_1\|_2^2 + b_1^2) + \frac{1}{2}\xi^T\xi + C_1\mathbf{e}^T\xi \\ \text{s.t.} & \mathbf{Y} - (\mathbf{A}\mathbf{w}_1 + b_1\mathbf{e}) = \xi, \\ & \mathbf{Y} - (\mathbf{A}\mathbf{w}_1 + b_1\mathbf{e}) \geq -\varepsilon_1\mathbf{e} - \xi, \xi \geq \mathbf{0}, \end{aligned}$$

and

$$\begin{aligned} \min_{\mathbf{w}_2, b_2, \xi^*} & \frac{1}{2}C_4(\|\mathbf{w}_2\|_2^2 + b_2^2) + \frac{1}{2}\xi^{*T}\xi^* + C_2\mathbf{e}^T\xi^* \\ \text{s.t.} & (\mathbf{A}\mathbf{w}_2 + b_2\mathbf{e}) - \mathbf{Y} = \xi^*, \\ & (\mathbf{A}\mathbf{w}_2 + b_2\mathbf{e}) - \mathbf{Y} \geq -\varepsilon_2\mathbf{e} - \xi^*, \xi^* \geq \mathbf{0}, \end{aligned}$$

where $C_3 > 0$, and $C_4 > 0$.

It can be seen that the function $f_1(x)$ determines the ε_1 -insensitive lower-bound regressor, and the function $f_2(x)$ determines the ε_2 -insensitive upper-bound regressor. Obviously, TSVR and ε -TSVR yield two nonparallel functions $f_1(x)$ and $f_2(x)$ to measure the asymmetric information of the training data set. However, TSVR and ε -TSVR are not suitable for the existence of heterogenous information in the training data points.

3. Twin support vector quantile regression

In this section, we bring the spirit of quantile regression into twin support vector regression, and then propose a twin support vector quantile regression (TSVQR) that takes unobserved heterogeneity and asymmetry into consideration. In the following, we will first propose a linear TSVQR, and then discuss the model property of TSVQR. Finally, we extend linear TSVQR into a nonlinear version.

3.1. Linear twin support vector quantile regression

3.1.1. Problem formulation

The goal of TSVQR is to find the following pair of lower-bound and upper-bound functions

$$f_1(x) = \mathbf{w}_1^T x + b_1,$$

and

$$f_2(x) = \mathbf{w}_2^T x + b_2.$$

The final decision function is constructed as

$$f(\mathbf{x}) = \frac{1}{2}(f_1(\mathbf{x}) + f_2(\mathbf{x})).$$

The minimization problems of TSVQR are as follows

$$\begin{aligned} \min_{\mathbf{w}_1, b_1, \xi} \quad & \frac{1}{2}(\|\mathbf{w}_1\|_2^2 + b_1^2) + C_1 \mathbf{e}^T \xi + C_1 \tau \mathbf{e}^T (\mathbf{Y} - \mathbf{A} \mathbf{w}_1 - b_1 \mathbf{e}) \\ \text{s.t.} \quad & \mathbf{Y} - (\mathbf{A} \mathbf{w}_1 + b_1 \mathbf{e}) \geq \varepsilon_1 \mathbf{e} - \xi, \quad \xi \geq \mathbf{0}, \end{aligned} \quad (4)$$

and

$$\begin{aligned} \min_{\mathbf{w}_2, b_2, \xi^*} \quad & \frac{1}{2}(\|\mathbf{w}_2\|_2^2 + b_2^2) + C_2 \mathbf{e}^T \xi^* + C_2 (1 - \tau) \mathbf{e}^T (\mathbf{A} \mathbf{w}_2 + b_2 \mathbf{e} - \mathbf{Y}) \\ \text{s.t.} \quad & (\mathbf{A} \mathbf{w}_2 + b_2 \mathbf{e}) - \mathbf{Y} \geq \varepsilon_2 \mathbf{e} - \xi^*, \quad \xi^* \geq \mathbf{0}, \end{aligned} \quad (5)$$

where $C_1 > 0$, $C_2 > 0$, ξ and ξ^* are the slack variables, $\varepsilon_1 > 0$ **and** $\varepsilon_2 > 0$ are parameters, and τ ($0 < \tau < 1$) is a quantile parameter.

It can be seen from (4) and (5) that the proposed TSVQR controls the negative influence of the training error on the final decision function by adjusting the quantile parameter τ . As τ increases from 0 to 1, the final decision function $f(x)$ moves up through the training data. Therefore, TSVQR effectively depicts the heterogeneous information at each quantile level of the training data points. Moreover, TSVQR comprises a pair of quadratic programming problems such that each QPP determines the either of the lower-bound or upper-bound functions by using one group of constraints. Specifically, given the quantile parameter and the training data set, function $f_1(x)$ determines the ε_1 -insensitive lower-bound regressor, while function $f_2(x)$ determines the ε_2 -insensitive upper-bound regressor. Obviously, $f_1(x)$ and $f_2(x)$ are nonparallel. Therefore, TSVQR effectively depicts the asymmetric information at each quantile level. TSVQR only solves two small-sized QPPs and each QPP has one group of constraints which reduces the computational complexity.

3.1.2. Problem solution

Define $\mathbf{G} = [\mathbf{A} \ \mathbf{e}]$, $\mathbf{u}_1 = [\mathbf{w}_1^T \ b_1]^T$, and $\mathbf{u}_2 = [\mathbf{w}_2^T \ b_2]^T$. The Lagrangian functions for the problems (4) and (5) are as follows

$$\begin{aligned} L(\mathbf{u}_1, \xi, \alpha, \beta) = & \frac{1}{2} \|\mathbf{u}_1\|_2^2 + C_1 \mathbf{e}^T \xi + C_1 \tau \mathbf{e}^T (\mathbf{Y} - \mathbf{u}_1^T \mathbf{G}) \\ & - \alpha^T (\mathbf{Y} - \mathbf{u}_1^T \mathbf{G} - \varepsilon_1 \mathbf{e} + \xi) - \beta^T \xi, \end{aligned}$$

and

$$L(\mathbf{u}_2, \xi^*, \alpha^*, \beta^*) = \frac{1}{2} \|\mathbf{u}_2\|_2^2 + C_2 \mathbf{e}^T \xi^* + C_2(1 - \tau) \mathbf{e}^T (\mathbf{u}_2^T \mathbf{G} - \mathbf{Y}) \\ - \alpha^{*T} (\mathbf{u}_2^T \mathbf{G} - \mathbf{Y} - \varepsilon_2 \mathbf{e} + \xi^*) - \beta^{*T} \xi^*,$$

where α , β , α^* , and β^* are the Lagrangian multiplier vectors. The KKT necessary and sufficient optimality conditions for the problems (4) and (5) are given by

$$\begin{aligned} \mathbf{u}_1 - C_1 \tau \mathbf{G}^T \mathbf{e} + \mathbf{G}^T \alpha &= 0, \\ C_1 \mathbf{e} - \alpha - \beta &= 0, \\ \mathbf{Y} - \mathbf{u}_1^T \mathbf{G} &\geq \varepsilon_1 \mathbf{e} - \xi, \quad \xi \geq \mathbf{0}, \\ \alpha^T (\mathbf{Y} - \mathbf{u}_1^T \mathbf{G} - \varepsilon_1 \mathbf{e} + \xi) &= 0, \quad \alpha \geq \mathbf{0}, \\ \beta^T \xi &= 0, \quad \beta \geq \mathbf{0}, \end{aligned} \tag{6}$$

and

$$\begin{aligned} \mathbf{u}_2 + C_2(1 - \tau) \mathbf{G}^T \mathbf{e} - \mathbf{G}^T \alpha^* &= 0, \\ C_2 \mathbf{e} - \alpha^* - \beta^* &= 0, \\ \mathbf{u}_2^T \mathbf{G} - \mathbf{Y} &\geq \varepsilon_2 \mathbf{e} - \xi^*, \quad \xi^* \geq \mathbf{0}, \\ \alpha^{*T} (\mathbf{u}_2^T \mathbf{G} - \mathbf{Y} - \varepsilon_2 \mathbf{e} + \xi^*) &= 0, \quad \alpha^* \geq \mathbf{0}, \\ \beta^{*T} \xi^* &= 0, \quad \beta^* \geq \mathbf{0}. \end{aligned} \tag{7}$$

Using the above KKT conditions, we obtain the following dual representations of optimization problems (4) and (5)

$$\begin{aligned} \min_{\alpha} \quad & \frac{1}{2} \alpha^T \mathbf{G} \mathbf{G}^T \alpha - C_1 \tau \mathbf{e}^T \mathbf{G} \mathbf{G}^T \alpha + \mathbf{Y}^T \alpha - \varepsilon_1 \mathbf{e}^T \alpha \\ \text{s.t.} \quad & \mathbf{0} \leq \alpha \leq C_1 \mathbf{e}, \end{aligned} \tag{8}$$

and

$$\begin{aligned} \min_{\alpha^*} \quad & \frac{1}{2} \alpha^{*T} \mathbf{G} \mathbf{G}^T \alpha^* - C_2(1 - \tau) \mathbf{e}^T \mathbf{G} \mathbf{G}^T \alpha^* - \mathbf{Y}^T \alpha^* - \varepsilon_2 \mathbf{e}^T \alpha^* \\ \text{s.t.} \quad & \mathbf{0} \leq \alpha^* \leq C_2 \mathbf{e}. \end{aligned} \tag{9}$$

We adopt the dual coordinate descent method (DCDM) (Hsieh et al., 2008) to solve problems (8) and (9). Define $\bar{\mathbf{G}} = \mathbf{G} \mathbf{G}^T$, $\mathbf{d}_1 = C_1 \tau \mathbf{G} \mathbf{G}^T \mathbf{e} -$

$\mathbf{Y} + \varepsilon_1 \mathbf{e}$, and $\mathbf{d}_2 = C_2(1 - \tau)\mathbf{G}\mathbf{G}^T \mathbf{e} + \mathbf{Y} + \varepsilon_2 \mathbf{e}$, (8) and (9) can be rewritten as

$$\begin{aligned} \min_{\alpha} f(\alpha) &= \frac{1}{2} \alpha^T \bar{\mathbf{G}} \alpha - \mathbf{d}_1^T \alpha \\ \text{s.t. } & \mathbf{0} \leq \alpha \leq C_1 \mathbf{e}, \end{aligned}$$

and

$$\begin{aligned} \min_{\alpha^*} f^*(\alpha^*) &= \frac{1}{2} \alpha^{*T} \bar{\mathbf{G}} \alpha^* - \mathbf{d}_2^T \alpha^* \\ \text{s.t. } & \mathbf{0} \leq \alpha^* \leq C_2 \mathbf{e}. \end{aligned}$$

The DCDM starts with a random initial points α^0 and α^{*0} , and for each iteration one of the variables is selected to minimize the following problems while the other variables are kept as constant solution

$$\begin{aligned} \min_{\mathbf{t}} f(\alpha_{\mathbf{i}} + tI_{\mathbf{i}}) \\ \text{s.t. } 0 \leq \alpha_{\mathbf{i}} + t \leq C_1, \quad i = 1, 2, \dots, l, \end{aligned} \tag{10}$$

and

$$\begin{aligned} \min_{\mathbf{t}^*} f^*(\alpha_{\mathbf{i}}^* + t^*I_{\mathbf{i}}) \\ \text{s.t. } 0 \leq \alpha_{\mathbf{i}}^* + t^* \leq C_2, \quad i = 1, 2, \dots, l, \end{aligned} \tag{11}$$

where I_i denotes the vector with 1 in the i -th coordinate and 0 elsewhere. The objective functions of (10) and (11) are simplified as

$$f(\alpha_{\mathbf{i}} + tI_{\mathbf{i}}) = \frac{1}{2} \bar{\mathbf{G}}_{ii} t^2 + \nabla_i f(\alpha_{\mathbf{i}}) t + f(\alpha_{\mathbf{i}}), \quad i = 1, 2, \dots, l,$$

and

$$f^*(\alpha_{\mathbf{i}}^* + t^*I_{\mathbf{i}}) = \frac{1}{2} \bar{\mathbf{G}}_{ii} t^{*2} + \nabla_i f^*(\alpha_{\mathbf{i}}^*) t^* + f^*(\alpha_{\mathbf{i}}^*), \quad i = 1, 2, \dots, l,$$

where $\nabla_i f$ and $\nabla_i f^*$ are the i -th components of the gradients ∇f and ∇f^* , respectively. Combining the bounded constraints $0 \leq \alpha_{\mathbf{i}} + t \leq C_1$ and $0 \leq \alpha_{\mathbf{i}}^* + t^* \leq C_2$, the minimizers of (10) and (11) lead to the following bounded constraint solutions

$$\alpha_{\mathbf{i}}^{new} = \min(\max(\alpha_{\mathbf{i}} - \frac{\nabla_i f(\alpha_{\mathbf{i}})}{\bar{\mathbf{G}}_{ii}}, 0), C_1),$$

and

$$\alpha_i^{*new} = \min(\max(\alpha_i^* - \frac{\nabla_i f^*(\alpha_i^*)}{\bar{\mathbf{G}}_{ii}}, 0), C_2).$$

The corresponding algorithm of linear TSVQR is summarized in Algorithm 1.

Algorithm 1: Dual coordinate descent algorithm for linear TSVQR.

Input: Training set (\mathbf{A}, \mathbf{Y}) ; Parameters $C_1, C_2, \tau, \varepsilon_1$ and ε_2 ;

Output: Updated α and α^* ;

begin

Set $\alpha = \mathbf{0}$ and $\alpha^* = \mathbf{0}$;

Compute $\mathbf{d} = C_1 \tau \mathbf{G} \mathbf{G}^T \mathbf{e} - \mathbf{Y} + \varepsilon_1 \mathbf{e}$,

$\mathbf{d}^* = C_2 (1 - \tau) \mathbf{G} \mathbf{G}^T \mathbf{e} + \mathbf{Y} + \varepsilon_2 \mathbf{e}$, and $\bar{\mathbf{G}} = \mathbf{G} \mathbf{G}^T$;

if α not converge; **then**

do for $i = 1, 2, \dots, l$ **do**

$\nabla_i f(\alpha_i) \leftarrow \alpha^T \bar{\mathbf{G}}_{ii} I_i - d^T I_i$

$\alpha_i^{old} \leftarrow \alpha_i$;

$\alpha_i \leftarrow \min(\max(\alpha_i - \frac{\nabla_i f(\alpha_i)}{\bar{\mathbf{G}}_{ii}}, 0), C_1)$;

end

if α^* not converge; **then**

do for $i = 1, 2, \dots, l$ **do**

$\nabla_i f(\alpha_i^*) \leftarrow \alpha^{*T} \bar{\mathbf{G}}_{ii} I_i - d^{*T} I_i$

$\alpha_i^{*old} \leftarrow \alpha_i^*$;

$\alpha_i^* \leftarrow \min(\max(\alpha_i^* - \frac{\nabla_i f^*(\alpha_i^*)}{\bar{\mathbf{G}}_{ii}}, 0), C_2)$;

end

end

By introducing the transformation from R^n to $R^{n+1} := \begin{bmatrix} x \\ 1 \end{bmatrix}$, the functions $f_1(x)$ and $f_2(x)$ can be expressed as

$$f_1(\mathbf{x}) = \mathbf{u}_1^\top \mathbf{x} = [\mathbf{w}_1^\top, b_1] \begin{bmatrix} x \\ 1 \end{bmatrix},$$

and

$$f_2(\mathbf{x}) = \mathbf{u}_2^\top \mathbf{x} = [\mathbf{w}_2^\top, b_1] \begin{bmatrix} x \\ 1 \end{bmatrix}.$$

Obtaining the solutions of α and α^* by Algorithm 1, the lower- and upper-bound functions $f_1(\mathbf{x})$ and $f_2(\mathbf{x})$ can be rewritten as

$$\begin{aligned} f_1(\mathbf{x}) &= \mathbf{u}_1^\top \mathbf{x} \\ &= C_1 \tau \mathbf{e}^T \mathbf{G} \mathbf{x} - \alpha^T \mathbf{G} \mathbf{x}, \end{aligned}$$

and

$$\begin{aligned} f_2(\mathbf{x}) &= \mathbf{u}_2^\top \mathbf{x} \\ &= -C_2(1 - \tau) \mathbf{e}^T \mathbf{G} \mathbf{x} + \alpha^{*T} \mathbf{G} \mathbf{x}. \end{aligned}$$

The final decision function is constructed as

$$\begin{aligned} f(\mathbf{x}) &= \frac{1}{2}(f_1(\mathbf{x}) + f_2(\mathbf{x})) \\ &= \frac{1}{2}(\alpha^* - \alpha)^T \mathbf{G} \mathbf{x} + \frac{1}{2}[C_1 \tau - C_2(1 - \tau)] \mathbf{e}^T \mathbf{G} \mathbf{x}. \end{aligned} \quad (12)$$

The first term in $f(\mathbf{x})$ is the sum of α and α^* , reflecting the asymmetric information at each quantile location of the training data points. The second term in $f(\mathbf{x})$, using the quantile parameter, depicts the heterogeneous information at each quantile level of the training data points. Therefore, TSVQR has the ability to solve the problems of heterogeneity and asymmetry.

3.1.3. Geometric interpretation

As the quantile parameter τ ranges from 0 to 1, we can obtain a family of $f_1(x)$, $f_2(x)$, and $f(x)$, respectively. We define the τ -th lower-bound function as $f_{1,\tau}(\mathbf{x})$, the upper-bound function as $f_{2,\tau}(\mathbf{x})$, and final decision function as $f_\tau(\mathbf{x})$. For simplicity of exposition, we focus on five cases where the values of τ are 0.10, 0.25, 0.50, 0.75, and 0.90, respectively. Then, we obtain the following down-bound functions

- (i) when $\tau = 0.10$, $f_1(x)$ becomes $f_{1,0.10}(\mathbf{x}) = 0.10C_1 \mathbf{e}^T \mathbf{G} \mathbf{x} - \alpha^T \mathbf{G} \mathbf{x}$,
- (ii) when $\tau = 0.25$, $f_1(x)$ becomes $f_{1,0.25}(\mathbf{x}) = 0.25C_1 \mathbf{e}^T \mathbf{G} \mathbf{x} - \alpha^T \mathbf{G} \mathbf{x}$,
- (iii) when $\tau = 0.50$, $f_1(x)$ becomes $f_{1,0.50}(\mathbf{x}) = 0.50C_1 \mathbf{e}^T \mathbf{G} \mathbf{x} - \alpha^T \mathbf{G} \mathbf{x}$,
- (iv) when $\tau = 0.75$, $f_1(x)$ becomes $f_{1,0.75}(\mathbf{x}) = 0.75C_1 \mathbf{e}^T \mathbf{G} \mathbf{x} - \alpha^T \mathbf{G} \mathbf{x}$,
- (v) when $\tau = 0.90$, $f_1(x)$ becomes $f_{1,0.90}(\mathbf{x}) = 0.90C_1 \mathbf{e}^T \mathbf{G} \mathbf{x} - \alpha^T \mathbf{G} \mathbf{x}$,

and the following up-bound functions

- (i) when $\tau = 0.10$, $f_2(x)$ becomes $f_{2,0.10}(\mathbf{x}) = \alpha^{*T} \mathbf{G} \mathbf{x} - 0.90C_2 \mathbf{e}^T \mathbf{G} \mathbf{x}$,
- (ii) when $\tau = 0.25$, $f_2(x)$ becomes $f_{2,0.25}(\mathbf{x}) = \alpha^{*T} \mathbf{G} \mathbf{x} - 0.75C_2 \mathbf{e}^T \mathbf{G} \mathbf{x}$,
- (iii) when $\tau = 0.50$, $f_2(x)$ becomes $f_{2,0.50}(\mathbf{x}) = \alpha^{*T} \mathbf{G} \mathbf{x} - 0.50C_2 \mathbf{e}^T \mathbf{G} \mathbf{x}$,
- (iv) when $\tau = 0.75$, $f_2(x)$ becomes $f_{2,0.75}(\mathbf{x}) = \alpha^{*T} \mathbf{G} \mathbf{x} - 0.25C_2 \mathbf{e}^T \mathbf{G} \mathbf{x}$,
- (v) when $\tau = 0.90$, $f_2(x)$ becomes $f_{2,0.90}(\mathbf{x}) = \alpha^{*T} \mathbf{G} \mathbf{x} - 0.10C_2 \mathbf{e}^T \mathbf{G} \mathbf{x}$.

We calculate the mean of $f_{1,\tau}(\mathbf{x})$ and $f_{2,\tau}(\mathbf{x})$, and obtain the following cases of $f_\tau(\mathbf{x})$.

Case 1: When $\tau = 0.10$, the final decision function (12) becomes

$$f_{\tau=0.10}(\mathbf{x}) = \frac{1}{2}(\alpha^* - \alpha)^T \mathbf{G}\mathbf{x} + \frac{1}{2}(0.1C_1 - 0.9C_2)\mathbf{e}^T \mathbf{G}\mathbf{x}.$$

$f_{\tau=0.10}(x)$ represents the conditional distribution of the training samples at the 0.1th quantile level.

Case 2: When $\tau = 0.25$, the final decision function (12) becomes

$$f_{\tau=0.25}(\mathbf{x}) = \frac{1}{2}(\alpha^* - \alpha)^T \mathbf{G}\mathbf{x} + \frac{1}{2}(0.25C_1 - 0.75C_2)\mathbf{e}^T \mathbf{G}\mathbf{x}.$$

$f_{\tau=0.25}(\mathbf{x})$ represents the conditional distribution of the training samples at first quantile.

Case 3: When $\tau = 0.50$, the final decision function (12) becomes

$$f_{\tau=0.50}(\mathbf{x}) = \frac{1}{2}(\alpha^* - \alpha)^T \mathbf{G}\mathbf{x} + \frac{1}{2}(0.5C_1 - 0.5C_2)\mathbf{e}^T \mathbf{G}\mathbf{x}.$$

$f_{\tau=0.50}(\mathbf{x})$ represents the conditional distribution of the training samples at median level.

Case 4: When $\tau = 0.75$, the final decision function (12) becomes

$$f_{\tau=0.75}(\mathbf{x}) = \frac{1}{2}(\alpha^* - \alpha)^T \mathbf{G}\mathbf{x} + \frac{1}{2}(0.75C_1 - 0.25C_2)\mathbf{e}^T \mathbf{G}\mathbf{x}.$$

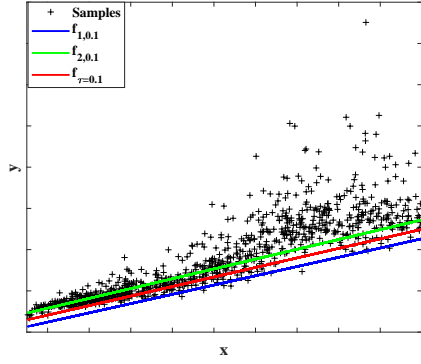
$f_{\tau=0.75}(\mathbf{x})$ represents the conditional distribution of the training samples at third quantile level.

Case 5: When $\tau = 0.90$, the final decision function (12) becomes

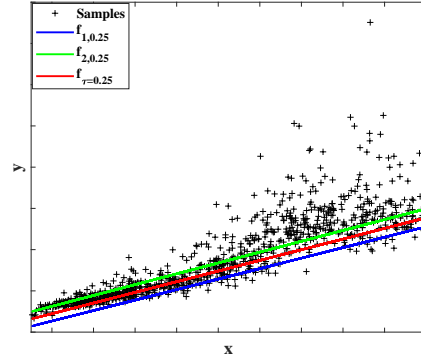
$$f_{\tau=0.90}(\mathbf{x}) = \frac{1}{2}(\alpha^* - \alpha)^T \mathbf{G}\mathbf{x} + \frac{1}{2}(0.9C_1 - 0.1C_2)\mathbf{e}^T \mathbf{G}\mathbf{x}.$$

$f_{\tau=0.90}(\mathbf{x})$ represents the conditional distribution of the training samples at the 0.9th quantile level.

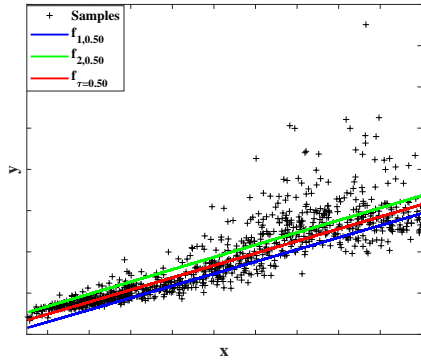
The intuitive geometric interpretation of TSVQR is shown in Fig. 1. The blue lines represent the lower-bound function $f_1(x)$ with different cases. The green lines represent the upper-bound function $f_2(x)$ with different cases. From Fig. 1 (a)-(e), we observe that $f_{1,\tau}(\mathbf{x})$ and $f_{2,\tau}(\mathbf{x})$ are nonparallel, demonstrating the information up and down the τ -th quantile location, respectively. Moreover, $f_{1,\tau}(\mathbf{x})$ and $f_{2,\tau}(\mathbf{x})$ adjust the quantile parameter to depict the whole distribution information, especially when unobservable heterogeneity exists in the training data points. The final decision function $f_\tau(\mathbf{x})$ in the middle of $f_{1,\tau}(\mathbf{x})$ and $f_{2,\tau}(\mathbf{x})$ is represented by the red lines in Fig. 1. Final decision functions provide a more complete picture of heterogeneous and asymmetric information in the training data points.



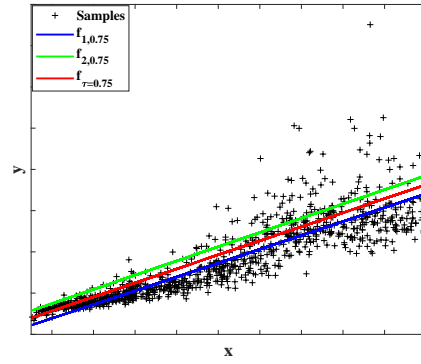
(a) $\tau = 0.10$



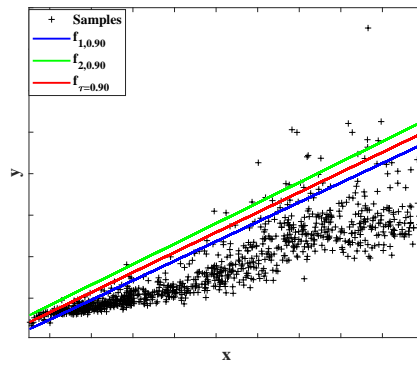
(b) $\tau = 0.25$



(c) $\tau = 0.50$



(d) $\tau = 0.75$



(e) $\tau = 0.90$

Figure 1: The geometric interpretation for TSVQR ($\tau = 0.10, 0.25, 0.50, 0.75, \text{ and } 0.90$).

3.2. Model property

3.2.1. Support vector

Theorem 1. Suppose that $\bar{\alpha} = (\bar{\alpha}_1, \dots, \bar{\alpha}_l)^T$ is the solution to (8) for $i = 1, \dots, l$, and $f_1(x) = \bar{\mathbf{w}}_1^\top x + \bar{b}_1$ is the optimal down-bound regression function.

(i) For $0 < \bar{\alpha}_i < C_1$, the corresponding data point (x_i, y_i) lies on the ε_1 -insensitive down-bound regressor.

(ii) For $\bar{\alpha}_i = C_1$, the corresponding data point (x_i, y_i) lies below the ε_1 -insensitive down-bound regressor.

(iii) For $\bar{\alpha}_i = 0$, the corresponding data point (x_i, y_i) lies above the ε_1 -insensitive down-bound regressor.

Proof. By KKT conditions (6), we obtain

$$\bar{\alpha} \in [\mathbf{0}, C_1 \mathbf{e}], \quad \bar{\alpha}^\top (\mathbf{Y} - \mathbf{A} \bar{\mathbf{w}}_1 - \bar{b}_1 \mathbf{e} - \varepsilon_1 \mathbf{e} + \bar{\xi}) = 0.$$

(i) If $\mathbf{0} < \bar{\alpha} < C_1 \mathbf{e}$, then $\mathbf{0} < \bar{\beta} < C_1 \mathbf{e}$, and $\bar{\xi} = \mathbf{0}$. We obtain $\mathbf{Y} = \bar{\mathbf{w}}_1^\top x + \bar{b}_1 \mathbf{e} + \varepsilon_1 \mathbf{e}$. For $0 < \bar{\alpha}_i < C_1$, the corresponding data point (x_i, y_i) lies on the ε_1 -insensitive down-bound regressor.

(ii) If $\bar{\alpha} = C_1 \mathbf{e}$, then $\bar{\beta} = \mathbf{0}$, and $\bar{\xi} > \mathbf{0}$. We obtain $\mathbf{Y} < \bar{\mathbf{w}}_1^\top x + \bar{b}_1 \mathbf{e} + \varepsilon_1 \mathbf{e}$. For $\bar{\alpha}_i = C_1$, the corresponding data point (x_i, y_i) lies below the ε_1 -insensitive down-bound regressor.

(iii) If $\bar{\alpha} = \mathbf{0}$, then $\bar{\beta} = C_1 \mathbf{e}$, and $\bar{\xi} = \mathbf{0}$. We obtain $\mathbf{Y} > \bar{\mathbf{w}}_1^\top x + \bar{b}_1 \mathbf{e} + \varepsilon_1 \mathbf{e}$. For $\bar{\alpha}_i = 0$, the corresponding data point (x_i, y_i) lies above the ε_1 -insensitive down-bound regressor. \square

Theorem 2. Suppose that $\bar{\alpha}^* = (\bar{\alpha}_1^*, \dots, \bar{\alpha}_l^*)^T$ is the solution to (9) for $i = 1, \dots, l$, and $f_2(x) = \bar{\mathbf{w}}_2^\top x + \bar{b}_2$ is the optimal up-bound regression function.

(i) For $0 < \bar{\alpha}_i^* < C_2$, the corresponding data point (x_i, y_i) lies on the ε_2 -insensitive up-bound regressor.

(ii) For $\bar{\alpha}_i^* = C_2$, the corresponding data point (x_i, y_i) lies above the ε_2 -insensitive up-bound regressor.

(iii) For $\bar{\alpha}_i^* = 0$, the corresponding data point (x_i, y_i) lies below the ε_2 -insensitive up-bound regressor.

Proof. By KKT conditions (7), we obtain

$$\bar{\alpha}^* \in [\mathbf{0}, C_2 \mathbf{e}], \quad \bar{\alpha}^{*\top} (\bar{\mathbf{w}}_2^\top x + \bar{b}_2 \mathbf{e} - \varepsilon_2 \mathbf{e} - \mathbf{Y} + \bar{\xi}^*) = 0.$$

(i) If $\mathbf{0} < \bar{\alpha}^* < C_2 \mathbf{e}$, then $\mathbf{0} < \bar{\beta}^* < C_2 \mathbf{e}$, and $\bar{\xi}^* = \mathbf{0}$. We obtain $\mathbf{Y} = \bar{\mathbf{w}}_2^\top x + \bar{b}_2 \mathbf{e} - \varepsilon_2 \mathbf{e}$. For $0 < \bar{\alpha}_i^* < C_2$, the corresponding data point (x_i, y_i) lies on the ε_2 -insensitive up-bound regressor.

- (ii) If $\bar{\alpha}^* = C_2\mathbf{e}$, then $\bar{\beta}^* = \mathbf{0}$, and $\bar{\xi}^* > \mathbf{0}$. We obtain $\mathbf{Y} > \bar{\mathbf{w}}_2^\top x + \bar{b}_2\mathbf{e} - \varepsilon_2\mathbf{e}$. For $\bar{\alpha}_i^* = C_2$, the corresponding data point (x_i, y_i) lies above the ε_2 -insensitive up-bound regressor.
- (iii) If $\bar{\alpha}^* = \mathbf{0}$, then $\bar{\beta}^* = C_2\mathbf{e}$, and $\bar{\xi}^* = \mathbf{0}$. We obtain $\mathbf{Y} < \bar{\mathbf{w}}_2^\top x + \bar{b}_2\mathbf{e} - \varepsilon_2\mathbf{e}$. For $\bar{\alpha}_i^* = 0$, the corresponding data point (x_i, y_i) lies below the ε_2 -insensitive up-bound regressor. \square

According to Theorems 1 and 2, we obtain

$$\left\{ \begin{array}{ll} y_i < \bar{\mathbf{w}}_1^\top x_i + \bar{b}_1 + \varepsilon_1, & \alpha_i = C_1, \\ y_i = \bar{\mathbf{w}}_1^\top x_i + \bar{b}_1 + \varepsilon_1, & 0 < \alpha_i < C_1, \\ \bar{\mathbf{w}}_1^\top x_i + \bar{b}_1 + \varepsilon_1 < y_i < \bar{\mathbf{w}}_2^\top x_i + \bar{b}_2 - \varepsilon_2, & \alpha_i = 0, \alpha_i^* = 0, \\ y_i = \bar{\mathbf{w}}_2^\top x_i + \bar{b}_2 - \varepsilon_2, & 0 < \alpha_i^* < C_2, \\ y_i > \bar{\mathbf{w}}_2^\top x_i + \bar{b}_2 - \varepsilon_2, & \alpha_i^* = C_2. \end{array} \right.$$

The index set of support vector in the TSVQR can be defined as $I_{SV} = \{i | 0 < \alpha_i \leq C_1, 0 < \alpha_i^* \leq C_2\}$.

3.2.2. Empirical Conditional Quantile Estimator

Proposition 1. *Let p , N , and Z denote the number of positive, negative, and zero elements of the residual vector $y_i - f(x_i)$. The minimizer of (4) and (5) satisfies:*

- (i) N is bounded from above by τl .
- (ii) p is bounded from above by $(1 - \tau)l$.
- (iii) If (x, y) is drawn iid from distribution $P(x, y)$, with $P(x, y)$ continuous and the expectation of the modulus of absolute continuity of its density satisfying $\lim_{\delta \rightarrow 0} E[\varepsilon(\delta)] = 0$. With probability 1, asymptotically, $\frac{N}{l}$ equals τ .

Proof. For the claims (i) and (ii), we follow the proof process of Takeuchi et al. (2006, Lemma 3) and Koenker (2005, Theorem 2.2). Assume that we get optimal solutions of (4) and (5). Then, increasing the minimizer f by δf changes the objective by $[N(1 - \tau) + Z(1 - \tau) - p\tau]\delta f$. Likewise, decreasing the minimizer f by δf changes the objective by $[-N(1 - \tau) + \tau p + \tau Z]\delta f$. Requiring that both terms are nonnegative at optimality in conjunction with the fact that $N + p \leq l$ and $l = N + p + Z$ prove the claims (i) and (ii).

For the claim (iii), we follow the proof process of Schölkopf (2000, Proposition 1). The condition on $P\{y|x\}$ means that

$$\sup_{f,t} E[P(|f(x) + t - y| < \gamma)] < \delta(\gamma). \quad (13)$$

When $\gamma \rightarrow 0$, function $\delta(\gamma)$ approaches 0. We further get that for all t

$$P(\sup_f(\hat{P}_l(|f(x) + t - y| < \gamma/2) < P(|f(x) + t - y| < \gamma)) > \alpha) < c_1 c_2^{-l},$$

where \hat{P}_l is the sample-based estimate of P , and c_1, c_2 may depend on γ and α . Discretizing the values of t , taking the union bound, and applying equation (13) show that the supremum over f and t of $\hat{P}_l(f(x) + t - y = 0)$ converges to 0 in probability. Thus, the fraction of points on the edge of the tube almost surely converges to 0. With probability 1, asymptotically, $\frac{N}{l}$ equals τ . \square

To illustrate regression analyses with the conditional quantile estimator, we provide the following example. Consider the relationship between y and x as

$$y(x) = \frac{\sin(2\pi x)}{2\pi x} + \xi, \xi \sim N(0, \sigma(x)^2),$$

where $\sigma(x) = 0.1e^{1+x}$, and $x \in [-1, 1]$. Compute the τ th quantiles by solving $P\{y \leq f|x\} = \tau$ explicitly. Since ξ is normally distributed, the τ th quantile of ξ is given by $\sigma(x)\phi^{-1}(\tau)$, where ϕ is the cumulative distribution function of the normal distribution with unit variance. We further get

$$y_\tau(x) = \frac{\sin(2\pi x)}{2\pi x} + 0.1e^{1+x}\phi^{-1}(\tau).$$

Fig. 2 shows the conditional quantile functions of (13) when $\tau = 0.10, 0.25, 0.50, 0.75,$ and 0.90 . The probability densities $p(y|x = -1), p(y|x = -0.5), p(y|x = 0), p(y|x = 0.5),$ and $p(y|x = 1)$ are also illustrated in Fig. 2. The τ th conditional quantile function is obtained by connecting the τ th quantile of the conditional distribution $p(y|x)$ for all x . From Fig. 2, we find that $\tau = 0.10, 0.25, 0.50, 0.75,$ and 0.90 cases track the lower, first quantile, median, third quantile, and upper envelope of the data points, respectively.

3.3. Nonlinear twin support vector quantile regression

For the nonlinear TSVQR, we first introduce a nonlinear mapping from the original space to the feature space: $\Phi \rightarrow \chi = \mathbf{\Phi}(\mathbf{X})$. The nonlinear regression functions are defined as follows

$$f_1(x) = \mathbf{w}_1^T \mathbf{\Phi}(x) + b_1,$$

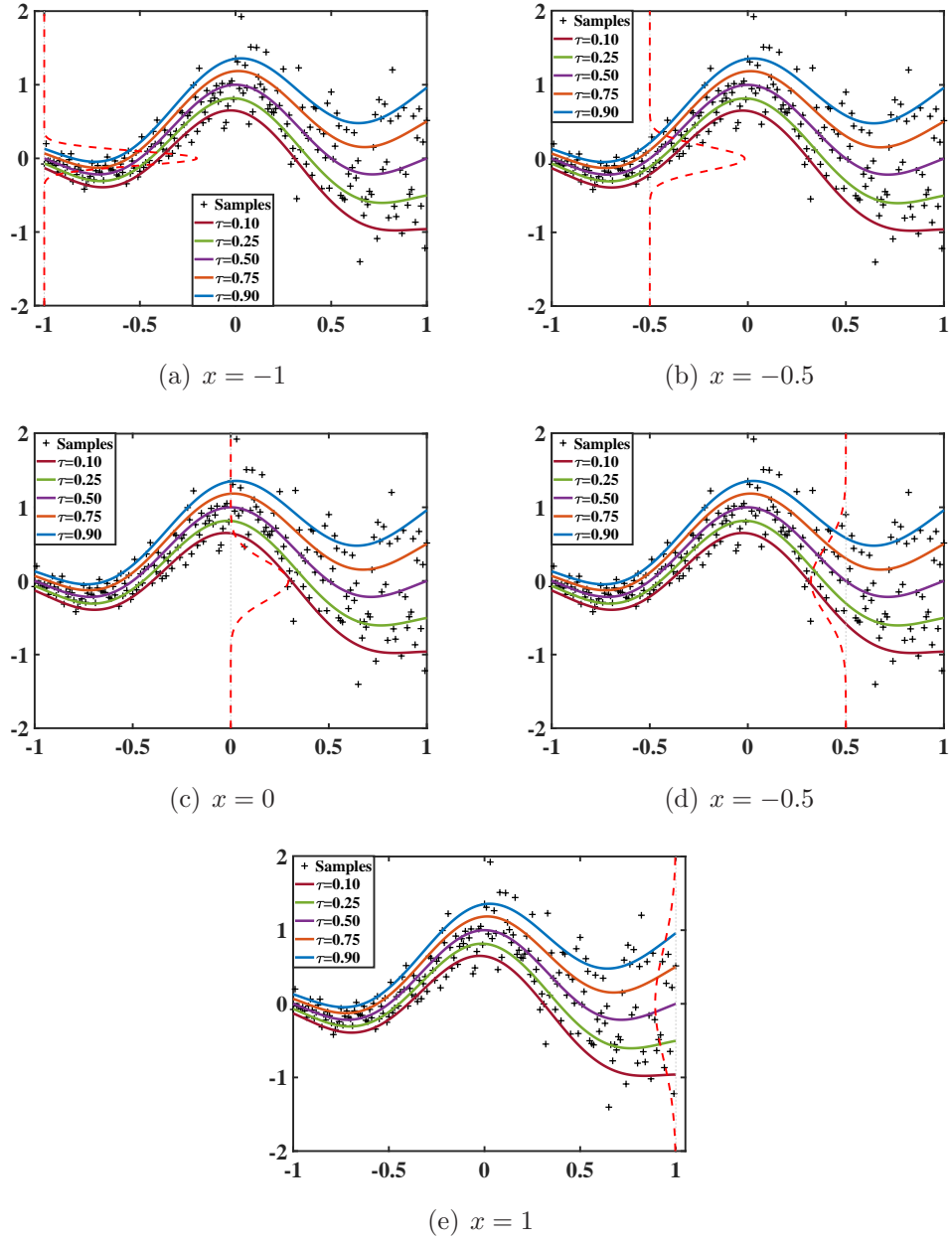


Figure 2: Conditional quantile functions and probability densities.

and

$$f_2(x) = \mathbf{w}_2^T \Phi(x) + b_2.$$

Similar to the linear case, the primal problems of the nonlinear TSVQR are as follows

$$\begin{aligned} \min_{\mathbf{w}_1, b_1, \xi} \quad & \frac{1}{2}(\|\mathbf{w}_1\|_2^2 + b_1^2) + C_1 \mathbf{e}^T \xi + C_1 \tau \mathbf{e}^T [\mathbf{Y} - \mathbf{w}_1^T \Phi(\mathbf{A}) - b_1 \mathbf{e}] \\ \text{s.t.} \quad & \mathbf{Y} - \mathbf{w}_1^T \Phi(\mathbf{A}) - b_1 \mathbf{e} \geq \varepsilon_1 \mathbf{e} - \xi, \quad \xi \geq \mathbf{0}, \end{aligned} \quad (14)$$

and

$$\begin{aligned} \min_{\mathbf{w}_2, b_2, \xi^*} \quad & \frac{1}{2}(\|\mathbf{w}_2\|_2^2 + \|b_2\|^2) + C_2 \mathbf{e}^T \xi^* + C_2(1 - \tau) \mathbf{e}^T [\mathbf{w}_2^T \Phi(\mathbf{A}) + b_2 \mathbf{e} - \mathbf{Y}] \\ \text{s.t.} \quad & \mathbf{w}_2^T \Phi(\mathbf{A}) + b_2 \mathbf{e} - \mathbf{Y} \geq \varepsilon_2 \mathbf{e} - \xi^*, \quad \xi^* \geq \mathbf{0}. \end{aligned} \quad (15)$$

Define $H = [\Phi(\mathbf{A}) \ \mathbf{e}]$, $\mathbf{u}_1 = [\mathbf{w}_1^T \ b_1]^T$, $\mathbf{u}_2 = [\mathbf{w}_2^T \ b_2]^T$. Then, we get the following Lagrangian functions of (14) and (15)

$$\begin{aligned} L(\mathbf{u}_1, \xi, \alpha, \beta) = & \frac{1}{2} \|\mathbf{u}_1\|_2^2 + C_1 \mathbf{e}^T \xi + C_1 \tau \mathbf{e}^T (\mathbf{Y} - \mathbf{u}_1^T \mathbf{H}) \\ & - \alpha^T (\mathbf{Y} - \mathbf{u}_1^T \mathbf{H} - \varepsilon_1 \mathbf{e} + \xi) - \beta^T \xi, \end{aligned}$$

and

$$\begin{aligned} L(\mathbf{u}_2, \xi^*, \alpha^*, \beta^*) = & \frac{1}{2} \|\mathbf{u}_2\|_2^2 + C_2 \mathbf{e}^T \xi^* + C_2(1 - \tau) \mathbf{e}^T (\mathbf{u}_2^T \mathbf{H} - \mathbf{Y}) \\ & - \alpha^{*T} (\mathbf{u}_2^T \mathbf{H} - \mathbf{Y} - \varepsilon_2 \mathbf{e} + \xi^*) - \beta^{*T} \xi^*, \end{aligned}$$

where α , β , α^* , and β^* are the Lagrangian multiplier vectors. The KKT necessary and sufficient optimality conditions for the problems (14) and (15) are given by

$$\begin{aligned} \mathbf{u}_1 - C_1 \tau \mathbf{H}^T \mathbf{e} + \mathbf{H}^T \alpha &= \mathbf{0}, \\ C_1 \mathbf{e} - \alpha - \beta &= \mathbf{0}, \\ \mathbf{Y} - \mathbf{u}_1^T \mathbf{H} &\geq \varepsilon_1 \mathbf{e} - \xi, \quad \xi \geq \mathbf{0}, \\ \alpha^T (\mathbf{Y} - \mathbf{u}_1^T \mathbf{H} - \varepsilon_1 \mathbf{e} + \xi) &= 0, \quad \alpha \geq \mathbf{0}, \\ \beta^T \xi &= \mathbf{0}, \quad \beta \geq \mathbf{0}, \end{aligned}$$

and

$$\begin{aligned} \mathbf{u}_2 + C_2(1 - \tau) \mathbf{H}^T \mathbf{e} - \mathbf{H}^T \alpha^* &= \mathbf{0}, \\ C_2 \mathbf{e} - \alpha^* - \beta^* &= \mathbf{0}, \\ \mathbf{u}_2^T \mathbf{H} - \mathbf{Y} &\geq \varepsilon_2 \mathbf{e} - \xi^*, \quad \xi^* \geq \mathbf{0}, \\ \alpha^{*T} (\mathbf{u}_2^T \mathbf{H} - \mathbf{Y} - \varepsilon_2 \mathbf{e} + \xi^*) &= 0, \quad \alpha^* \geq \mathbf{0}, \\ \beta^{*T} \xi^* &= \mathbf{0}, \quad \beta^* \geq \mathbf{0}. \end{aligned}$$

Using the above KKT conditions, we derive the dual problems of (14) and (15)

$$\begin{aligned} \min_{\alpha} \quad & \frac{1}{2}\alpha^{\mathbf{T}}\mathbf{H}\mathbf{H}^{\mathbf{T}}\alpha - C_1\tau\mathbf{e}^{\mathbf{T}}\mathbf{H}\mathbf{H}^{\mathbf{T}}\alpha + \mathbf{Y}^{\mathbf{T}}\alpha - \varepsilon_1\mathbf{e}^{\mathbf{T}}\alpha \\ \text{s.t.} \quad & \mathbf{0} \leq \alpha \leq C_1\mathbf{e}, \end{aligned} \quad (16)$$

and

$$\begin{aligned} \min_{\alpha^*} \quad & \frac{1}{2}\alpha^{*\mathbf{T}}\mathbf{H}\mathbf{H}^{\mathbf{T}}\alpha^* - C_2(1-\tau)\mathbf{e}^{\mathbf{T}}\mathbf{H}\mathbf{H}^{\mathbf{T}}\alpha^* - \mathbf{Y}^{\mathbf{T}}\alpha^* - \varepsilon_2\mathbf{e}^{\mathbf{T}}\alpha^* \\ \text{s.t.} \quad & \mathbf{0} \leq \alpha^* \leq C_2\mathbf{e}. \end{aligned} \quad (17)$$

Similarly, we use DCDM to solve problems (16) and (17). Define $\bar{\mathbf{H}} = \mathbf{H}\mathbf{H}^{\mathbf{T}} = \mathbf{K}(\mathbf{A}, \mathbf{A}^{\mathbf{T}}) + \mathbf{e}\mathbf{e}^{\mathbf{T}}$, $\mathbf{d}_1 = C_1\tau\mathbf{H}\mathbf{H}^{\mathbf{T}}\mathbf{e} - \mathbf{Y} + \varepsilon_1\mathbf{e}$, and $\mathbf{d}_2 = C_2(1-\tau)\mathbf{H}\mathbf{H}^{\mathbf{T}}\mathbf{e} + \mathbf{Y} + \varepsilon_2\mathbf{e}$. $\mathbf{K}(\mathbf{A}, \mathbf{A}^{\mathbf{T}}) = \Phi(\mathbf{A})\Phi(\mathbf{A}^{\mathbf{T}})$ is the kernel function. Then, (16) and (17) can be rewritten as

$$\begin{aligned} \min_{\alpha} \quad & f(\alpha) = \frac{1}{2}\alpha^{\mathbf{T}}\bar{\mathbf{H}}\alpha - \mathbf{d}_1^{\mathbf{T}}\alpha \\ \text{s.t.} \quad & \mathbf{0} \leq \alpha \leq C_1\mathbf{e}, \end{aligned}$$

and

$$\begin{aligned} \min_{\alpha^*} \quad & f^*(\alpha^*) = \frac{1}{2}\alpha^{*\mathbf{T}}\bar{\mathbf{H}}\alpha^* - \mathbf{d}_2^{\mathbf{T}}\alpha^* \\ \text{s.t.} \quad & \mathbf{0} \leq \alpha^* \leq C_2\mathbf{e}. \end{aligned}$$

DCDM starts with a random initial points α^0 and α^{*0} . For updating α and α^* , we solve the following one-variable sub-problems

$$\begin{aligned} \min_{\mathbf{t}} \quad & f(\alpha_i + tI_i) \\ \text{s.t.} \quad & 0 \leq \alpha_i + t \leq C_1, \quad i = 1, 2, \dots, l, \end{aligned} \quad (18)$$

and

$$\begin{aligned} \min_{\mathbf{t}^*} \quad & f^*(\alpha_i^* + t^*I_i) \\ \text{s.t.} \quad & 0 \leq \alpha_i^* + t^* \leq C_2, \quad i = 1, 2, \dots, l. \end{aligned} \quad (19)$$

The objective functions of (18) and (19) are simplified as

$$f(\alpha_i + tI_i) = \frac{1}{2}\bar{\mathbf{H}}_{ii}t^2 + \nabla_i f(\alpha_i)t + f(\alpha_i), \quad i = 1, 2, \dots, l,$$

and

$$f^*(\alpha_i^* + t^* I_i) = \frac{1}{2} \bar{\mathbf{H}}_{ii} t^{*2} + \nabla_i f^*(\alpha_i^*) t^* + f^*(\alpha_i^*), \quad i = 1, 2, \dots, l.$$

We combine the bounded constraints $0 \leq \alpha_i + t \leq C_1$ and $0 \leq \alpha_i^* + t^* \leq C_2$, and get the following bounded constraint solutions of (18) and (19)

$$\alpha_i^{new} = \min(\max(\alpha_i - \frac{\nabla_i f(\alpha_i)}{\bar{\mathbf{H}}_{ii}}, 0), C_1),$$

and

$$\alpha_i^{*new} = \min(\max(\alpha_i^* - \frac{\nabla_i f^*(\alpha_i^*)}{\bar{\mathbf{H}}_{ii}}, 0), C_2).$$

Then, we obtain Algorithm 2 to solve nonlinear TSVQR in detail. Finally, we obtain the down- and up-bound functions $f_1(x)$ and $f_2(x)$, and then construct the final decision function $f(x) = \frac{1}{2}[f_1(x) + f_2(x)]$. The flowchart of the solution of nonlinear TSVQR is summarized in Fig. 3.

3.4. Discussion

TSVQR follows the spirit of ε -TSVR (Shao et al., 2013), and generates two nonparallel functions to determine the ε -insensitive lower and upper bounds for capturing the asymmetric information in data points. Moreover, TSVQR brings the spirit of QR (Dempster et al., 1977) into TSVR, and uses the quantile parameter to compute a family of regression curves corresponding to various percentage points of the distributions. As the quantile parameter increases, the regression curves move up through the data to reflect the heterogeneous information in data points. TSVQR thus effectively captures the heterogeneous and asymmetric information in data points simultaneously.

Concerning the computational complexity of TSVQR, we find that the major computational cost of TSVQR comes from the kernel matrix. Note that \mathbf{A} is an $l \times n$ matrix. TSVQR and URALTSVR only solve two smaller-sized QPPs in which DCDM is applied. Thus, the computational complexity of Algorithm 2 is estimated as $2O(l^2)$. Although SVQR only solves one single QPP, the QPP in SVQR has two groups of constraints for all data. The computational complexity of SVQR, ε -SVQR, Online-SVQR and RQSVR is approximately $O(2l)^3$. Thus, TSVQR and URALTSVR work faster than SVQR, ε -SVQR, Online-SVQR, and RQSVR. Table 2 shows the important merit and demerit of SVQR, ε -SVQR, GPQR, Online-SVQR, RQSVR, URALTSVR, and TSVQR.

Algorithm 2: Dual coordinate descent algorithm for nonlinear TSVQR.

Input: Training set (\mathbf{A}, \mathbf{Y}) ; Parameters $C_1, C_2, \tau, \varepsilon_1$ and ε_2 , and the kernel parameter P ;

Output: Updated α and α^* ;

begin

Set $\alpha = \mathbf{0}$ and $\alpha^* = \mathbf{0}$;

Compute $\mathbf{d} = C_1\tau\mathbf{H}\mathbf{H}^T\mathbf{e} - \mathbf{Y} + \varepsilon_1\mathbf{e}$,

$\mathbf{d}^* = C_2(1 - \tau)\mathbf{H}\mathbf{H}^T\mathbf{e} + \mathbf{Y} + \varepsilon_2\mathbf{e}$, and $\bar{\mathbf{H}} = \mathbf{H}\mathbf{H}^T$;

if α not converge; **then**

do for $i = 1, 2, \dots, l$ do

$\nabla_i f(\alpha_i) \leftarrow \alpha^T \bar{\mathbf{H}}_{ii} I_i - d^T I_i$

$\alpha_i^{old} \leftarrow \alpha_i$;

$\alpha_i \leftarrow \min(\max(\alpha_i - \frac{\nabla_i f(\alpha_i)}{\bar{\mathbf{H}}_{ii}}, 0), C_1)$;

end

if α^* not converge; **then**

do for $i = 1, 2, \dots, l$ do

$\nabla_i f(\alpha_i^*) \leftarrow \alpha^{*T} \bar{\mathbf{H}}_{ii} I_i - d^{*T} I_i$

$\alpha_i^{*old} \leftarrow \alpha_i^*$;

$\alpha_i^* \leftarrow \min(\max(\alpha_i^* - \frac{\nabla_i f^*(\alpha_i^*)}{\bar{\mathbf{H}}_{ii}}, 0), C_2)$;

end

end

Table 2: The merit and demerit of SVQR, ε -SVQR, GPQR, Online-SVQR, RQSVR, URALTSVR, and TSVQR.

Methods	Merits	Demerits/ Limitations
SVQR (Li et al., 2007)	<ul style="list-style-type: none"> Using the quantile parameter. 	<ul style="list-style-type: none"> High computation time due to large QPP. Does not solve the asymmetry problem.
ε -SVQR (Anand et al., 2020)	<ul style="list-style-type: none"> Using the quantile parameter. Using ε-insensitive loss. 	<ul style="list-style-type: none"> High computation time due to large QPP. Does not solve the asymmetry problem.
GPQR (Ouhourane et al., 2022)	<ul style="list-style-type: none"> Using the quantile parameter. Sparseness. 	<ul style="list-style-type: none"> Does not solve the asymmetry problem.
Online-SVQR (Ye et al., 2021)	<ul style="list-style-type: none"> Using the quantile parameter. Using ε-insensitive loss. Reflecting the dynamic information. 	<ul style="list-style-type: none"> High computation time due to large QPP. Does not solve the asymmetry problem.
RQSVR (Yang & Dong, 2019)	<ul style="list-style-type: none"> Using pinball loss function. Robustness. 	<ul style="list-style-type: none"> High computation time due to large QPP. Does not solve the asymmetry problem.
URALTSVR (Gupta & Gupta, 2021a)	<ul style="list-style-type: none"> Using pinball loss function. Less computation time by using the gradient based iterative approaches. Controlling the fitting error inside the asymmetric tube. 	<ul style="list-style-type: none"> Lack of sparseness.
TSVQR	<ul style="list-style-type: none"> Using ε-insensitive loss. Depicting heterogenous information. Reflecting asymmetric information. Fast processing by solving two small QPPs. 	<ul style="list-style-type: none"> Lack of sparseness.

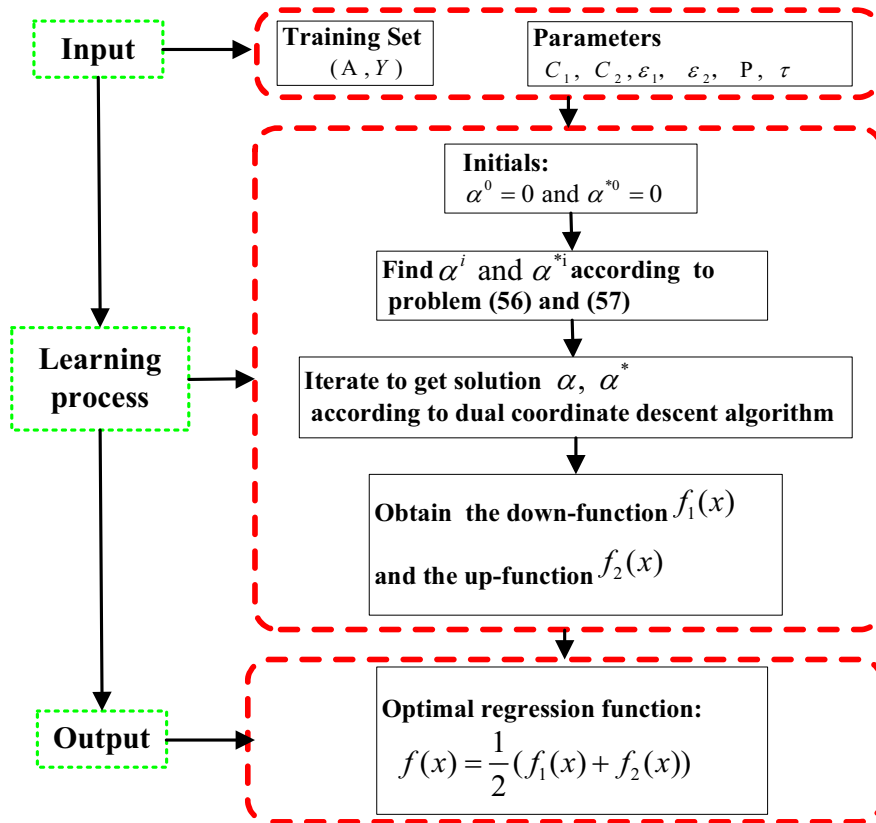


Figure 3: Flowchart of the solution of nonlinear TSVQR.

4. Experiments

To test the efficiency of the proposed TSVQR, we compare with SVQR, ε -SVQR, Online-SVQR, GPQR, RQSVR, URALTSVR, and least squares large margin distribution machine-based regression (LS-LDMR) (Gupta & Gupta, 2021b) on several data sets, including six artificial data sets and five benchmark data sets. All of these methods are implemented in the MATLAB R2021a environment on a PC running the 64-bit Windows XP OS and 16 GB of RAM.

4.1. Performance criteria

Suppose m is the number of testing samples, y_i^t is the i th test sample, \hat{y}_i^t is the predicted value of y_i^t , and $\bar{y}^t = \frac{1}{m} \sum_{i=1}^m y_i^t$ is the average value of y_1^t, \dots, y_m^t . For the nonlinear version of TSVQR, we employ a Gaussian kernel, and its kernel parameter P is selected from the set $\{2^{-8}, \dots, 2^8\}$. Parameters C_1 and C_2 are selected from the set $\{2^{-8}, \dots, 2^8\}$. The quantile parameter is chosen from the set $\{0.10, 0.25, 0.50, 0.75, 0.90\}$. The insensitive parameters ε_1 and ε_2 are chosen from 0.01 to 0.1 with a fixed step size of 0.01. The optimal values of the parameters in our experiments are obtained by using the grid search method. We use the generalized approximate cross validation (GACV) criterion (Yuan, 2006; Xu et al., 2015) to select the optimal values of the parameters. The definition of GACV is as follows

$$GACV_\tau = \frac{1}{l-|I_{SV}|} \sum_{i=1}^l \rho_\tau(y_i^t - \hat{y}_i^t)$$

where $|I_{SV}|$ is the cardinality of the set I_{SV} , and $\rho_\tau(r)$ is the pinball loss function of Koenker and Bassett (1978)

$$\rho_\tau(r) = \begin{cases} \tau r, & \text{if } r > 0, \\ -(1 - \tau)r, & \text{otherwise.} \end{cases}$$

To evaluate the performance of the proposed method, we use the following evaluation criteria, namely the empirical quantile risk (Risk), the root mean square error (RMSE), the mean absolute error (MAE) and the mean absolute percentage error (MAPE). These evaluation criteria are defined as follows

$$\text{Risk}_\tau = \frac{1}{m} \sum_{i=1}^m \rho_\tau(y_i^t - \hat{y}_i^t),$$

Table 3: Function used for generating artificial data sets.

Function definition	Domain of definition	Noise type
$y = (1 - x + 2x^2)e^{-0.5x^2} + \frac{1}{5}(1 + 0.2x)\xi$	$x \in [-4, 4]$	Type A_1 : $\xi_i \sim \chi^2(3)$
		Type A_2 : $\xi_i \sim \chi^2(5)$
		Type A_3 : Laplacian Noise
$y = 6\sin(0.5\pi - x) + 3(\sin(0.5\pi - x))\xi$	$x \in [-4, 4]$	Type B_1 : $\xi_i \sim N(0.3, 0.6^2)$
		Type B_2 : $\xi_i \sim N(0.5, 0.8^2)$
		Type B_3 : Laplacian Noise

$$\text{RMSE} = \sqrt{\frac{1}{m} \sum_{i=1}^m (y_i^t - \hat{y}_i^t)^2},$$

$$\text{MAE} = \frac{1}{m} \sum_{i=1}^m |y_i^t - \hat{y}_i^t|,$$

$$\text{MAPE} = \frac{\sum_{i=1}^m |y_i^t - \hat{y}_i^t| / y_i^t}{m}.$$

4.2. Artificial data sets

We first construct six artificial data sets to test the performance of TSVQR whose definitions are given in Table 3. The specifications of these artificial data sets are listed in Table 4. The training samples of Type A_3 and Type B_3 contain outliers. According to the values of GACV, we select the best parameters of TSVQR, and then list them in Table 5.

Tables 6-11 show the regression results of SVQR, ϵ -SVQR, Online-SVQR, GPQR and TSVQR when $\tau = 0.10, 0.25, 0.50, 0.75,$ and 0.90 , and their corresponding regression performance is depicted in Figs. 4-7. Table 12 shows the regression results of LS-LDMR, RQSVR and URALTSVR. From these tables, we see that TSVQR achieves smaller Risk, RMSE, MAE, and MAPE than those of SVQR, ϵ -SVQR, Online-SVQR and GPQR in most cases, which means that TSVQR fits the data set at every quantile location. From Figs. 4-7, we observe that there is a significant distributional heterogeneity at each data set. In Figs. 4-7, the dotted lines represent the final decision function of LS-LDMR, RQSVR, and URALTSVR, respectively. These dotted lines

Table 4: Descriptive statistics of data sets.

Data set	Number of training samples	Number of testing samples
Type A_1	401	400
Type A_2	401	400
Type A_3	405	400
Type B_1	801	161
Type B_2	801	161
Type B_3	805	400
Engel	187	48
Bone density	388	97
US girls	3209	802
Motorcycle	99	33
Boston housing	405	101

Table 5: The optimal parameters selected of artificial data sets by GACV.

τ	0.10	0.25	0.50	0.75	0.90
Type A_1					
C_1	2^3	2^3	2^3	2^{-2}	2^3
C_2	2^3	2^3	2^3	2^{-2}	2^3
P	2^0	2^0	2^0	2^0	2^0
Type A_2					
C_1	2^3	2^3	2^3	2^1	2^3
C_2	2^3	2^3	2^3	2^1	2^3
P	2^0	2^0	2^0	2^0	2^0
Type A_3					
C_1	2^3	2^3	2^3	2^3	2^3
C_2	2^3	2^3	2^3	2^3	2^3
P	2^0	2^0	2^0	2^0	2^0
Type B_1					
C_1	2^1	2^2	2^1	2^3	2^3
C_2	2^1	2^2	2^1	2^3	2^3
P	2^1	2^1	2^1	2^1	2^1
Type B_2					
C_1	2^1	2^2	2^1	2^3	2^3
C_2	2^1	2^2	2^1	2^3	2^3
P	2^1	2^1	2^1	2^1	2^1
Type B_3					
C_1	2^3	2^3	2^2	2^3	2^3
C_2	2^3	2^3	2^2	2^3	2^3
P	2^1	2^1	2^1	2^1	2^1

are located in the middle of the training data sets, which reflect the mean of the conditional distribution of the training data set. SVQR, ϵ -SVQR, Online-SVQR, GPQR and TSVQR depict the distribution of the training data set at different quantile locations. Comparing with the regression results of SVQR, ϵ -SVQR, Online-SVQR, and GPQR in Figs. 4-7, we find that TSVQR effectively explores the distribution information at each quantile level. TSVQR uses a pair of nonparallel bound functions to depict the distribution information up and down each quantile level. Therefore, TSVQR can effectively capture the heterogeneous and asymmetric information over the whole training data set. Moreover, for the CPU time in Tables 6-11, the training speed of TSVQR and URALTSVR is much faster than that of SVQR, ϵ -SVQR, Online-SVQR, and GPQR since TSVQR and URALTSVR only solve two small QPPs in the learning process.

4.3. Benchmark data sets

In this subsection, we consider five benchmark data sets to demonstrate the efficacy of TSVQR. The benchmark data sets include “Engel” (Koenker & Bassett Jr, 1982), “Bone density” (Bachrach et al., 1999), “US girls” (Cole, 1988), “Motorcycle” (Härdle, 1990), and “Boston housing” (Harrison Jr & Rubinfeld, 1978). The “Engel” data set illustrates the relationship between food expenditure and household income increases. The “Bone density” data set presents the relationship between age and bone mineral density. The “US girls” data set demonstrates the relationship between age and weight for US girls. The “Boston housing” data set and “Motorcycle” data set are very popular in the UC Irvine (UCI) Machine Learning Repository. These five real-world data sets are very popular in QR studies. The specifications of these standardized real-world data sets are listed in Table 4. We adopt a meta-analysis to quantify the degree of heterogeneity of these five real-world data sets. Typically, in meta-analysis, heterogeneity is assessed with the I^2 index (Higgins & Thompson, 2002). All the heterogeneity tests of these real-world data sets are implemented in Stata 15.1. I^2 values of 25%, 50%, and 75% are interpreted as representing low, moderate, and high levels of heterogeneity, respectively. “Engel”, “Bone density”, “US girls”, “Motorcycle” and “Boston housing” I^2 values are 0%, 0%, 77.4%, 98.7%, and 100%, respectively. These values indicate that “US girls”, “Motorcycle” and “Boston housing” reflect great heterogeneity. The I^2 values of “Engel” and “Bone density” are 0, indicating that there is no heterogeneity.

Table 6: Comparison results of SVQR, ϵ -SVQR, Online-SVQR, GPQR, and TSVQR for artificial data set Type A_1 .

Indices	SVQR	ϵ -SVQR	Online-SVQR	GPQR	TSVQR
$\tau = 0.10$					
Risk	0.5695	0.5890	0.5732	0.0956	0.0325
RMSE	0.6808	0.7020	0.6914	0.3847	0.0669
MAE	0.6344	0.6551	0.6447	0.2899	0.0404
MAPE	0.4721	0.4780	0.4761	0.3875	0.0789
CPU Time	0.3056	0.1822	0.2439	0.1671	0.0220
$\tau = 0.25$					
Risk	0.3698	0.3719	0.3708	0.1734	0.0352
RMSE	0.5334	0.5361	0.5347	0.3609	0.0648
MAE	0.4941	0.4969	0.4955	0.2681	0.0517
MAPE	0.3847	0.3858	0.3853	0.3610	0.0760
CPU Time	0.1748	0.1781	0.1765	0.1488	0.0271
$\tau = 0.50$					
Risk	0.0504	0.0957	0.0723	0.2278	0.0369
RMSE	0.1190	0.2049	0.1587	0.5054	0.0937
MAE	0.1008	0.1914	0.1446	0.4555	0.0738
MAPE	0.1035	0.1713	0.1392	0.4345	0.0786
CPU Time	0.2045	0.1845	0.1945	0.2292	0.0216
$\tau = 0.75$					
Risk	0.0335	0.0328	0.0321	0.1970	0.0302
RMSE	0.1041	0.1298	0.1154	0.8546	0.1202
MAE	0.0871	0.1084	0.0958	0.7878	0.1017
MAPE	0.0732	0.0894	0.0782	0.5374	0.0981
CPU Time	0.1440	0.1726	0.1583	0.1306	0.0202
$\tau = 0.90$					
Risk	0.1307	0.1195	0.1250	0.1207	0.0380
RMSE	0.2040	0.1947	0.1992	0.6067	0.4034
MAE	0.1625	0.1530	0.3644	0.8514	0.1575
MAPE	0.1414	0.1324	0.1367	0.6151	0.2036
CPU Time	0.1860	0.1845	0.1853	0.1346	0.0331

Table 7: Comparison results of SVQR, ϵ -SVQR, Online-SVQR, GPQR, and TSVQR for artificial data set Type A_2 .

Indices	SVQR	ϵ -SVQR	Online-SVQR	GPQR	TSVQR
$\tau = 0.10$					
Risk	0.8024	0.9554	0.9583	0.2361	0.2199
RMSE	0.9612	0.8015	0.8045	0.4721	0.2647
MAE	1.0680	1.0616	1.0648	0.3756	0.2444
MAPE	0.5715	0.5703	0.5709	0.4053	0.2865
CPU Time	0.0811	0.0848	0.0829	0.1217	0.0205
$\tau = 0.25$					
Risk	0.6374	0.6523	0.6448	0.3513	0.2622
RMSE	0.8973	0.9153	0.9063	0.6262	0.3968
MAE	0.8499	0.8697	0.8598	0.4801	0.3496
MAPE	0.4889	0.4938	0.4913	0.4219	0.2949
CPU Time	0.0751	0.0693	0.0722	0.1260	0.0154
$\tau = 0.50$					
Risk	0.2403	0.3697	0.3050	0.4319	0.2149
RMSE	0.5317	0.7728	0.6522	0.8850	0.4906
MAE	0.4805	0.7394	0.6099	0.8638	0.4298
MAPE	0.3104	0.4080	0.3592	0.5395	0.2796
CPU Time	0.0721	0.0548	0.0634	0.1422	0.0163
$\tau = 0.75$					
Risk	0.0969	0.3011	0.1990	0.3173	0.0576
RMSE	0.4733	0.4878	0.4805	0.5694	0.3985
MAE	0.3877	0.4044	0.3961	0.5118	0.3305
MAPE	0.2195	0.2290	0.2242	0.6189	0.3194
CPU Time	0.0800	0.0726	0.0763	0.1220	0.0198
$\tau = 0.90$					
Risk	0.1111	0.6079	0.3595	0.1843	0.1055
RMSE	0.4383	0.4393	0.4388	0.9443	0.5821
MAE	0.3804	0.3803	0.3803	0.8426	0.5549
MAPE	0.2245	0.2228	0.2237	0.6846	0.4016
CPU Time	0.0674	0.0622	0.0648	0.1335	0.0154

The optimal parameters of TSVQR for benchmark data sets are shown in Table 13. Tables 14-18 list the regression results of real-world data sets for SVQR, ϵ -SVQR, Online-SVQR, GPQR and TSVQR, when $\tau = 0.10, 0.25, 0.50, 0.75,$ and 0.90 , and their corresponding regression performance is depicted in Figs. 8-11. Table 19 shows the regression results of benchmark data sets for LS-LDMR, RQSVR and URALTSVR. From Fig. 8, we observe the tendency of the dispersion of food expenditure to increase along with increases in the level of household income, indicating the heterogeneous

Table 8: Comparison results of SVQR, ϵ -SVQR, Online-SVQR, GPQR, and TSVQR for artificial data set Type A_3 .

Indices	SVQR	ϵ -SVQR	Online-SVQR	GPQR	TSVQR
$\tau = 0.10$					
Risk	0.1500	0.1441	0.3169	0.0902	0.0844
RMSE	0.4063	0.4104	0.5835	1.0130	0.0995
MAE	0.3407	0.3456	0.4132	0.9015	0.1712
MAPE	0.4772	0.5431	0.6207	1.9459	2.6641
CPU Time	0.1721	0.1311	0.2671	0.4606	0.0263
$\tau = 0.25$					
Risk	0.1187	0.1168	0.2175	0.1346	0.1051
RMSE	0.3665	0.3700	0.5724	0.6122	0.3602
MAE	0.3082	0.3101	0.5097	0.4985	0.5005
MAPE	0.3598	0.3686	0.3648	1.8338	2.4293
CPU Time	0.1813	0.1376	0.1949	0.1896	0.0263
$\tau = 0.50$					
Risk	0.1217	0.3411	0.2341	0.3205	0.0193
RMSE	0.3102	0.7080	0.5221	0.0677	0.4103
MAE	0.2542	0.6821	0.4681	0.0410	0.3927
MAPE	0.3837	3.2275	1.2341	0.1877	0.1672
CPU Time	0.1308	0.1465	0.1865	0.2447	0.0280
$\tau = 0.75$					
Risk	0.5925	0.5457	0.4691	0.3687	0.2682
RMSE	0.8146	0.7543	0.8045	0.3334	0.2038
MAE	0.7900	0.7276	0.7588	0.2746	0.3576
MAPE	2.4777	2.4599	2.2729	0.3498	0.2951
CPU Time	0.1454	0.1136	0.1713	0.2076	0.0280
$\tau = 0.90$					
Risk	0.6778	0.6657	0.6219	0.0613	0.1498
RMSE	0.7997	0.7870	0.7989	0.6774	0.2490
MAE	0.7531	0.7396	0.7411	0.6621	0.1981
MAPE	2.8441	3.3715	1.3019	0.6127	0.1510
CPU Time	0.1544	0.1647	0.1927	0.2779	0.0288

statistical features in the “Engel” data set. From Fig. 8(e), we find that different income groups have different marginal propensities for food expenditure. Combining the regression results in Table 14, we see that TSVQR and GPQR yield a smaller Risk than SVQR, ϵ -SVQR, and Online-SVQR in most cases. This means that the statistical information at different quantile levels is well presented by TSVQR since the empirical quantile risk (Risk) uses the quantile parameter to measure the information capturing ability at different quantile levels. For the CPU time in Table 14, we find that the training

Table 9: Comparison results of SVQR, ε -SVQR, Online-SVQR, GPQR, and TSVQR for artificial data set Type B_1 .

Indices	SVQR	ε -SVQR	Online-SVQR	GPQR	TSVQR
$\tau = 0.10$					
Risk	1.8635	1.8564	1.8600	0.1095	0.1169
RMSE	2.2745	2.2673	2.2709	0.7385	0.4595
MAE	2.0706	2.0627	2.0666	0.9052	0.4163
MAPE	1.1695	1.1337	1.1507	0.2619	0.1465
CPU Time	0.5707	0.5485	0.5597	0.5360	0.1058
$\tau = 0.25$					
Risk	0.9243	0.9026	0.9135	0.3901	0.2748
RMSE	1.4754	1.4459	1.4606	0.9114	0.5362
MAE	1.2645	1.2392	1.2518	0.6984	0.4677
MAPE	0.8868	0.9090	0.7760	0.5653	0.1467
CPU Time	0.4838	0.5072	0.4966	0.5487	0.1023
$\tau = 0.50$					
Risk	0.2994	0.2508	0.2715	0.2932	0.2356
RMSE	0.7004	0.5860	0.6387	0.6416	0.5362
MAE	0.5987	0.5015	0.5430	0.5864	0.4711
MAPE	0.2081	0.1421	0.2454	0.4292	0.1000
CPU Time	0.4423	0.4479	0.4451	0.5635	0.1141
$\tau = 0.75$					
Risk	0.3458	0.2240	0.2716	0.2514	0.2174
RMSE	0.7250	0.7488	0.6806	0.6952	0.5583
MAE	0.6131	0.6489	0.6044	0.4890	0.4882
MAPE	0.7131	0.2335	0.1618	0.3114	0.1112
CPU Time	0.6067	0.5626	0.5849	0.5001	0.0957
$\tau = 0.90$					
Risk	0.5434	0.5102	0.5265	0.1527	0.1892
RMSE	0.9540	0.9248	0.9390	0.6802	0.5999
MAE	0.7220	0.7079	0.7143	0.6785	0.5392
MAPE	0.2483	0.2826	0.2497	0.6192	0.1883
CPU Time	0.5612	0.5520	0.5566	0.4627	0.0878

speed of TSVQR is faster than those of SVQR, ε -SVQR, Online-SVQR, and GPQR as TSVQR only solves two smaller-sized QPPs without any equality constraint in the learning process and the dual coordinate descent algorithm is adopted to solve the QPPs. Figs. 9-11 demonstrate that TSVQR depicts more complete pictures of training data set than SVQR, ε -SVQR, and Online-SVQR. The results in Tables 15-19 also confirm the effectiveness of TSVQR to demonstrate the heterogeneous statistical information in the data sets. Moreover, it can be seen that the differences between TSVQR and the

Table 10: Comparison results of SVQR, ε -SVQR, Online-SVQR, GPQR, and TSVQR for artificial data set Type B_2 .

Indices	SVQR	ε -SVQR	Online-SVQR	GPQR	TSVQR
$\tau = 0.10$					
Risk	0.8239	0.9657	0.8948	0.2348	0.5496
RMSE	1.0961	0.9510	1.0235	0.5847	0.3121
MAE	0.8429	0.8039	0.8234	0.3485	0.2223
MAPE	0.9661	0.5475	0.7568	0.7149	0.4299
CPU Time	0.4793	0.3701	0.4247	0.6505	0.0651
$\tau = 0.25$					
Risk	0.9851	0.8427	0.9139	0.3192	0.1688
RMSE	0.8509	0.8712	0.8610	0.6930	0.3874
MAE	0.8991	1.0362	0.9676	0.7768	0.5366
MAPE	0.9127	0.8616	0.8871	0.5741	0.2337
CPU Time	0.3526	0.4066	0.3796	0.5200	0.0687
$\tau = 0.50$					
Risk	0.3633	0.3420	0.3526	0.2432	0.3184
RMSE	0.8180	0.7866	0.8023	0.5587	0.5172
MAE	0.7266	0.6840	0.7053	0.4865	0.2369
MAPE	0.2834	0.3691	0.3262	0.1039	0.1371
CPU Time	0.3232	0.3053	0.3143	0.5921	0.0970
$\tau = 0.75$					
Risk	0.4423	0.4905	0.4664	0.2415	0.1817
RMSE	0.9532	0.8955	0.9243	0.9447	0.6772
MAE	0.8279	0.7721	0.8000	0.9661	0.7074
MAPE	0.2829	0.3863	0.3346	0.4356	0.2396
CPU Time	0.3400	0.3707	0.3554	0.5307	0.0797
$\tau = 0.90$					
Risk	0.7038	0.7005	0.7021	0.2050	0.1359
RMSE	0.9762	0.7047	0.8404	1.0640	0.5817
MAE	0.7466	0.5750	0.6608	2.0498	0.3588
MAPE	0.4351	0.4347	0.4349	0.6808	0.1042
CPU Time	0.3820	0.3660	0.3741	0.5149	0.0713

other seven models with respect to RMSE and MAE are not significant. The main reason is that neither definition adopts the quantile parameter τ . Therefore, it is worth exploring more reasonable criteria to evaluate quantile regression results in our future work. Regarding the training speed, we find that the training speed of TSVQR, LS-LDMR, and URALTSVR is also the fastest in all cases.

Table 11: Comparison results of SVQR, ε -SVQR, Online-SVQR, GPQR, and TSVQR for artificial data set Type B_3 .

Indices	SVQR	ε -SVQR	Online-SVQR	GPQR	TSVQR
$\tau = 0.10$					
Risk	2.1839	1.9878	1.0231	0.5974	0.5162
RMSE	2.7531	2.5632	2.1413	1.1216	1.1991
MAE	2.4266	2.2093	1.8937	1.0744	1.0247
MAPE	1.4777	1.7382	1.1591	0.6817	0.3095
CPU Time	0.4376	0.4182	0.6279	1.4200	0.0837
$\tau = 0.25$					
Risk	1.3821	1.1999	1.2291	0.7580	0.6428
RMSE	2.1900	1.9404	2.1253	0.7710	1.2376
MAE	2.8604	1.6517	2.2601	0.7347	1.1106
MAPE	1.9190	1.9529	1.7376	0.6171	0.2654
CPU Time	0.4353	0.4441	0.4809	0.5822	0.0803
$\tau = 0.50$					
Risk	0.6098	2.2063	0.8193	0.5116	0.5139
RMSE	1.3695	1.0971	1.8129	0.5373	1.1227
MAE	1.2197	0.3278	0.9142	0.5233	1.0278
MAPE	0.4109	1.2063	0.8633	0.5076	0.2451
CPU Time	0.3170	0.3722	0.5542	0.5798	0.0701
$\tau = 0.75$					
Risk	1.0659	0.6193	0.8127	0.6632	0.4638
RMSE	1.4655	0.1287	2.1234	0.7881	1.1820
MAE	1.3193	1.0923	2.0051	0.7567	1.0691
MAPE	0.5185	0.4985	0.5087	0.5163	0.2782
CPU Time	0.3931	0.4879	0.7409	0.5970	0.0734
$\tau = 0.90$					
Risk	1.0652	1.0827	1.2711	0.5589	0.3324
RMSE	2.0803	1.6964	1.8160	1.1437	1.0690
MAE	1.9389	1.3087	1.0717	1.0895	1.1969
MAPE	1.3047	1.4091	1.7522	0.6974	0.4182
CPU Time	0.3599	0.3892	0.7461	0.6487	0.0734

4.4. Statistical test

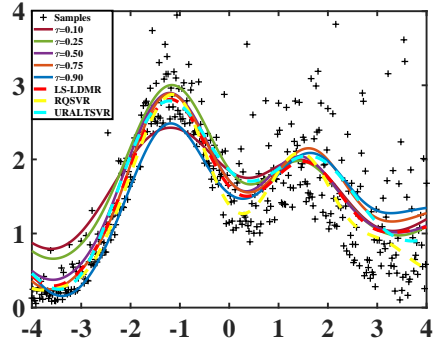
To fairly evaluate the experimental results of SVQR, ε -SVQR, Online-SVQR, GPQR, and TSVQR on six artificial data sets and five benchmark data sets, we adopt the Friedman test (Demšar, 2006; Ye et al., 2020). Table 20 lists the Friedman test results of SVQR, ε -SVQR, Online-SVQR, GPQR, and TSVQR. At the 10% significance level, the critical values of $\chi^2(4)$ and $F(4, 32)$ are 7.78 and 2.14, respectively. From Table 20, we find that the χ^2 and F_F values of the Risk and the CPU time at different quantile levels are

Table 12: Evaluation indices of artificial data sets for LS-LDMR, RQSVR and URALTSVR.

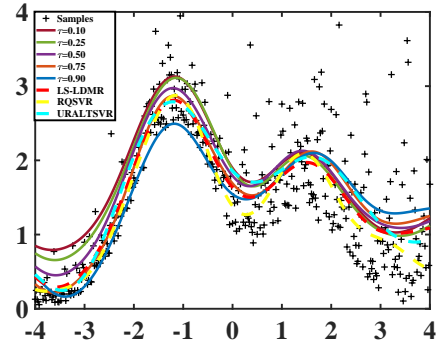
Data set	Method	RMSE	MAE	MAPE	CPU Time
Type A_1	LS-LDMR	0.1989	0.1779	0.1698	0.0105
	RQSVR	0.5117	0.4694	0.4447	0.3569
	URALTSVR	0.7020	0.6451	1.5015	0.0232
Type A_2	LS-LDMR	0.6205	0.5676	0.3470	0.0023
	RQSVR	0.9370	0.8502	0.5468	0.1075
	URALTSVR	1.1316	1.0343	0.5848	0.0212
Type A_3	LS-LDMR	0.2603	0.2056	0.2811	0.0220
	RQSVR	0.0875	0.0539	0.1826	0.1051
	URALTSVR	0.2096	0.1832	0.3077	0.0253
Type B_1	LS-LDMR	0.6332	0.5698	0.1343	0.0249
	RQSVR	0.6240	0.5791	0.1287	0.4437
	URALTSVR	0.6490	0.5956	0.1274	0.1352
Type B_2	LS-LDMR	0.7257	0.6527	0.1469	0.0113
	RQSVR	0.4769	0.4114	0.0940	0.4419
	URALTSVR	0.5532	0.5028	0.1218	0.0781
Type B_3	LS-LDMR	4.3206	3.9747	0.2171	0.0074
	RQSVR	0.0477	0.0368	0.0111	0.2999
	URALTSVR	0.1471	0.1088	0.0546	0.0829

much greater than their corresponding critical values. Therefore, the null hypothesis is failed to acceptance level that means all five methods are not equivalent to each other.

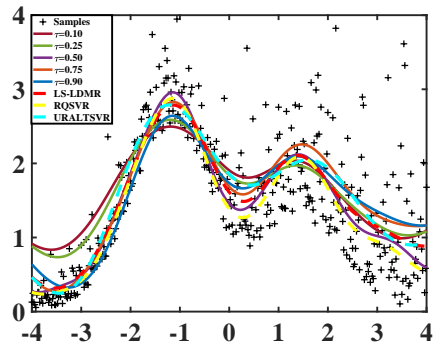
We further use Nemenyi test (Demšar, 2006; Ye et al., 2020) to compare SVQR, ε -SVQR, Online-SVQR, GPQR, and TSVQR in terms of the Risk and the CPU time. The critical value of Nemenyi test at the 10% significance level is 1.8328. Nemenyi test results for the Risk and the CPU time are list in Table 21. From Table 21, we find that the differences between TSVQR and other models with respect to the Risk are larger than 1.8328 in most cases. Let us compare TSVQR with SVQR, ε -SVQR, and Online-SVQR. When $\tau = 0.10$, the difference values are 2.0000, 2.3636, and 2.2727, respectively, which are more than 1.8328. It is evident that regression performance of TSVQR is superior to SVQR, ε -SVQR, and Online-SVQR. When $\tau = 0.90$, we can get the same conclusion. For the running time, we find that the training speed of TSVQR is significantly faster than SVQR, Online-SVQR, and GPQR in all cases, since the difference between them is larger than the critical value.



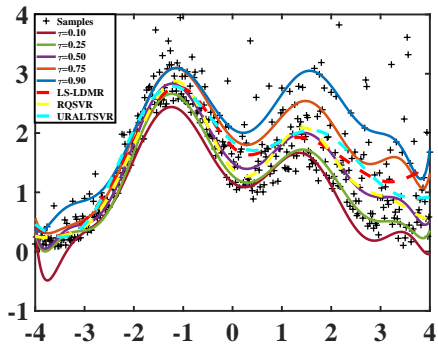
(a) SVQR



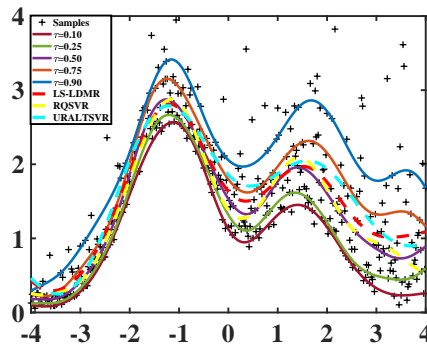
(b) ε -SVQR



(c) Online-SVQR

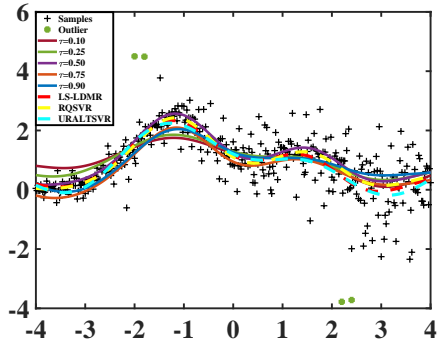


(d) GPQR

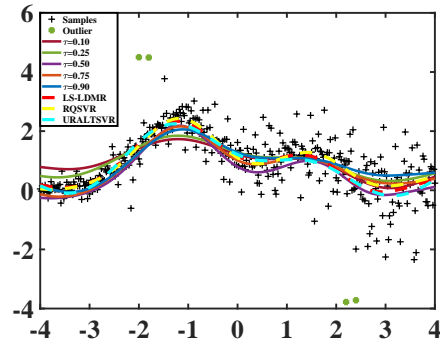


(e) TSVQR

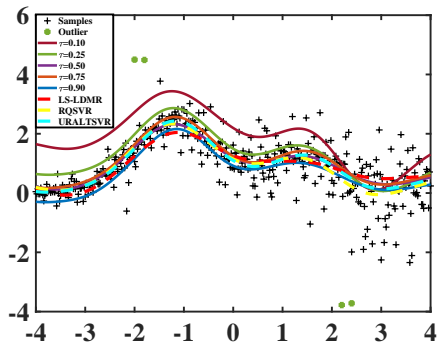
Figure 4: Regression results of SVQR, ε -SVQR, Online-SVQR, GPQR, TSVQR, LS-LDMR, RQSVR, and URALTSVR for Type A_1 .



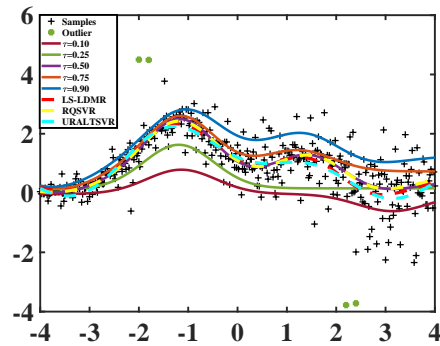
(a) SVQR



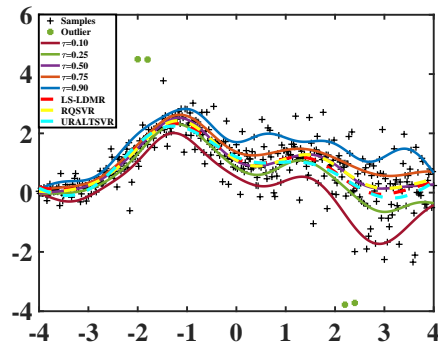
(b) ε -SVQR



(c) Online-SVQR



(d) GPQR



(e) TSVQR

Figure 5: Regression results of SVQR, ε -SVQR, Online-SVQR, GPQR, TSVQR, LS-LDMR, RQSVR, and URALTSVR for Type A_3 .

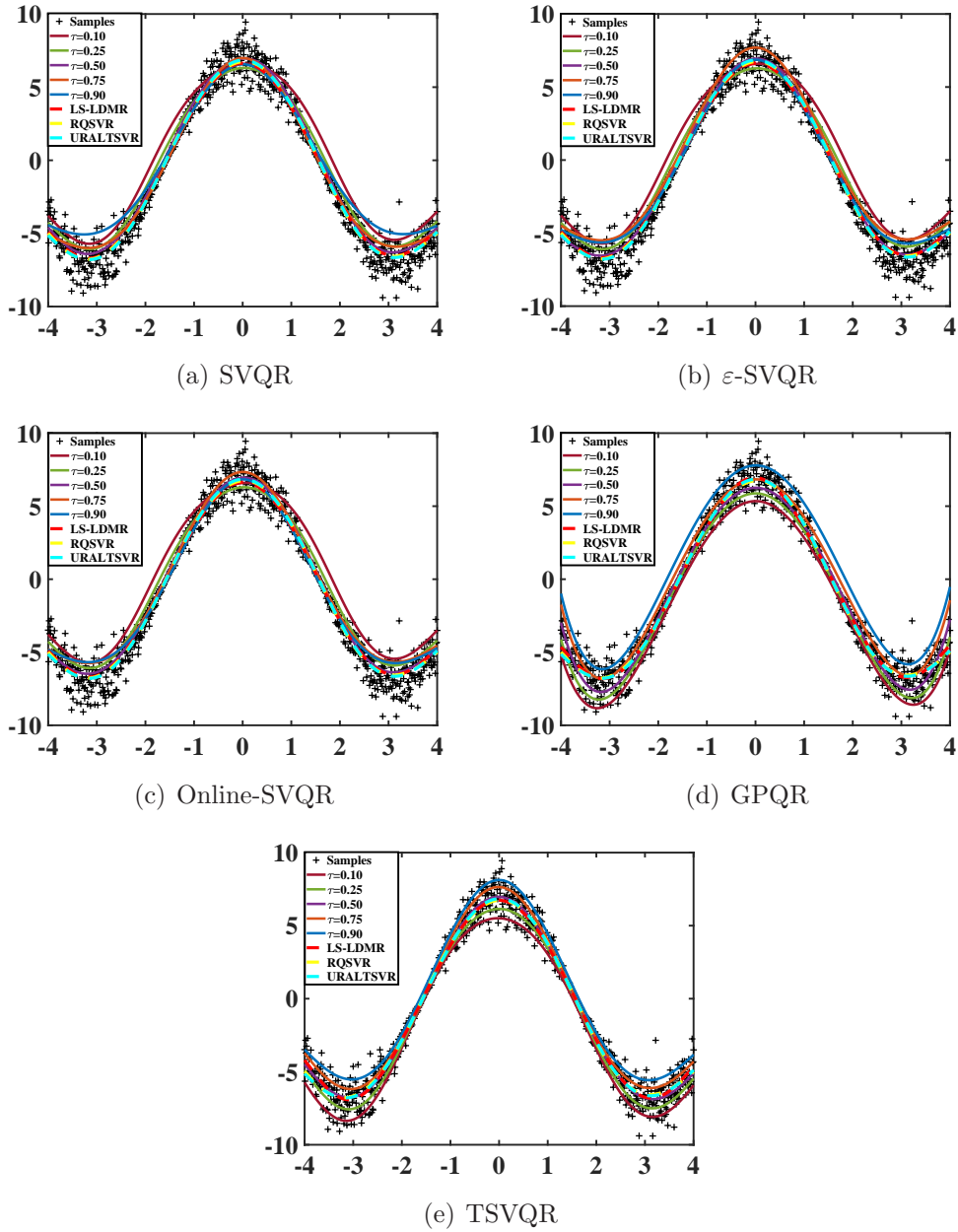


Figure 6: Regression results of SVQR, ε -SVQR, Online-SVQR, GPQR, TSVQR, LS-LDMR, RQSVR, and URALTSVR for Type B_1 .

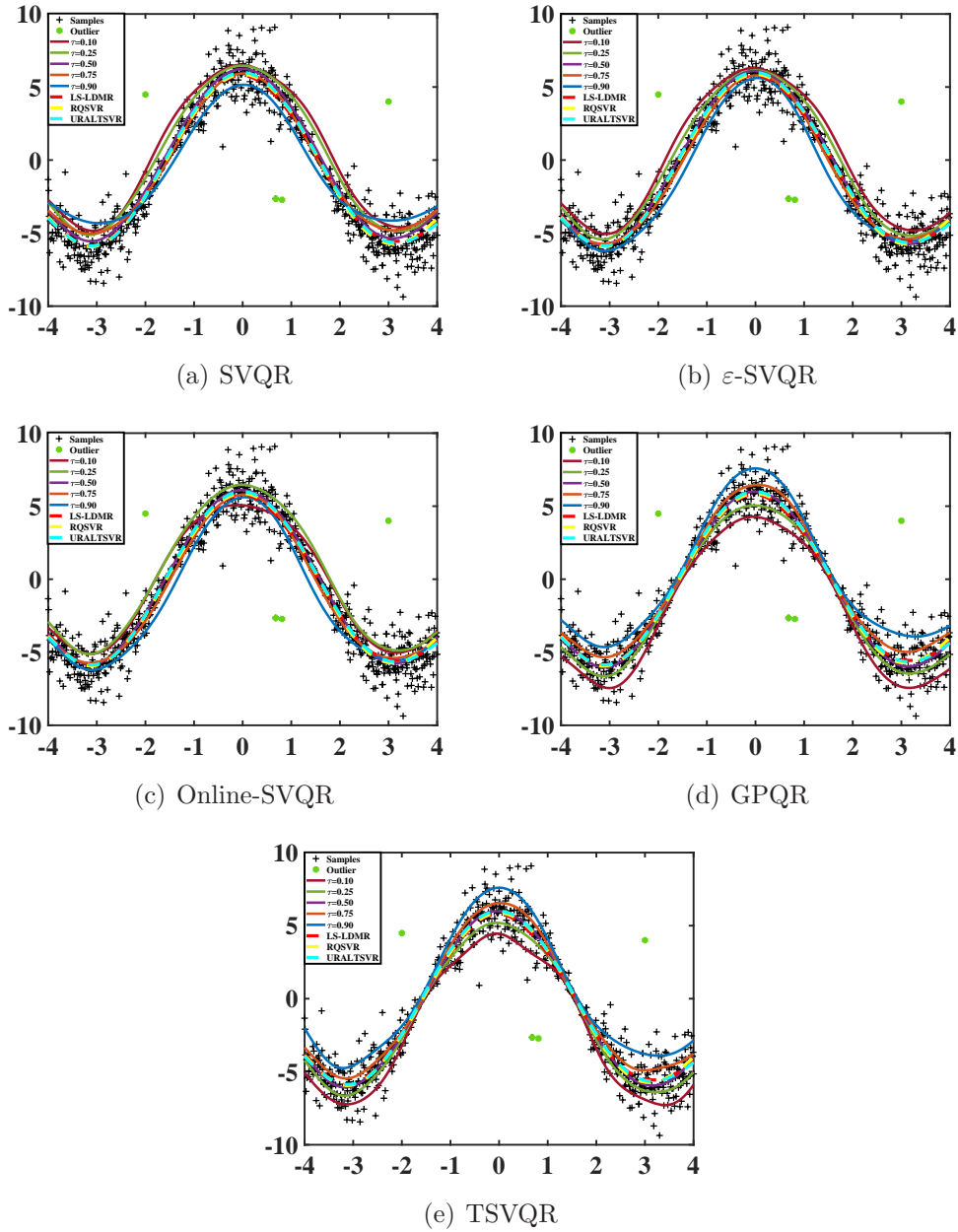


Figure 7: Regression results of SVQR, ε -SVQR, Online-SVQR, GPQR, TSVQR, LS-LDMR, RQSVR, and URALTSVR for Type B_3 .

Table 13: The optimal parameters of Benchmark data sets selected by GACV.

τ	0.10	0.25	0.50	0.75	0.90
Engel					
C ₁	2 ⁻¹	2 ⁻¹	2 ⁻¹	2 ⁻¹	2 ⁻¹
C ₂	2 ⁻¹	2 ⁻¹	2 ⁻¹	2 ⁻¹	2 ⁻¹
P	2 ⁰	2 ⁰	2 ⁰	2 ⁰	2 ⁰
Bone density					
C ₁	2 ⁻²	2 ⁻²	2 ⁻²	2 ⁻²	2 ⁻²
C ₂	2 ⁻²	2 ⁻²	2 ⁻²	2 ⁻²	2 ⁻²
P	2 ⁰	2 ⁰	2 ⁰	2 ⁰	2 ⁰
US girls					
C ₁	2 ⁻²	2 ⁻²	2 ⁻²	2 ⁻²	2 ⁻²
C ₂	2 ⁻²	2 ⁻²	2 ⁻²	2 ⁻²	2 ⁻²
P	2 ¹	2 ¹	2 ¹	2 ¹	2 ¹
Motorcycle					
C ₁	2 ⁻¹	2 ⁻¹	2 ⁻¹	2 ⁻¹	2 ⁻¹
C ₂	2 ⁻¹	2 ⁻¹	2 ⁻¹	2 ⁻¹	2 ⁻¹
P	2 ⁻¹	2 ⁻¹	2 ⁻¹	2 ⁻¹	2 ⁻¹
Boston housing					
C ₁	2 ⁻¹	2 ⁻¹	2 ⁻¹	2 ⁻¹	2 ⁻¹
C ₂	2 ⁻¹	2 ⁻¹	2 ⁻¹	2 ⁻¹	2 ⁻¹
P	2 ⁰	2 ⁰	2 ⁰	2 ⁰	2 ⁰

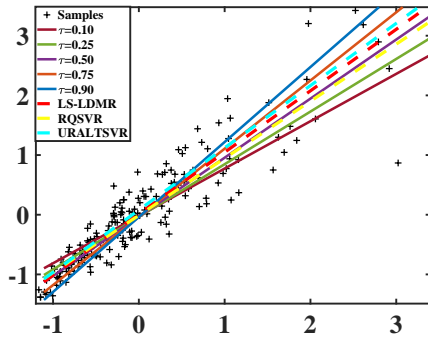
We further adopt Friedman test to evaluate the training speed of LS-LDMR, URALTSVR, RQSVR, SVQR, ε -SVQR, Online-SVQR, GPQR, and TSVQR. The χ^2 value of CPU time is 57.88, which is larger than the critical value 14.067 at the 5% significance level. It can be concluded that the null hypothesis is rejected and all eight approaches are concluded to be not equivalent. The Nemenyi test has been applied for pairwise comparative analysis on SVQR, ε -SVQR, Online-SVQR, GPQR, TSVQR, LS-LDMR, RQSVR and URALTSVR. Tabel 22 lists the results of the Nemenyi test. Comparing the training speed of LS-LDMR with SVQR, ε -SVQR, Online-SVQR, GPQR, and RQSVR, we find the difference values are 5.4545, 4.2727, 5.2727, 4.9090, and 3.4545, respectively, which are more than the critical value 2.69 at the 5% significance level, indicating that the training speed of LS-LDMR is superior to SVQR, ε -SVQR, Online-SVQR, GPQR, and RQSVR. Checking the difference of LS-LDMR with URALTSVR and TSVQR, we find that their difference values are 1.0909 and 1.3636, respectively, which are less than the critical value 2.69. Therefore, there is no significant difference between the training speed of LS-LDMR, URALTSVR and TSVQR.

Table 14: Evaluation indices of Engel data set.

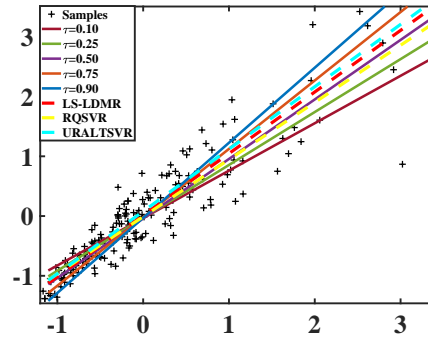
τ	Method	Risk	RMSE	MAE	CPU Time
0.10	SVQR	0.1888	0.4983	0.3809	0.2224
	ε -SVQR	0.1925	0.4983	0.3786	0.0520
	Online-SVQR	0.4258	1.2055	0.7492	0.1373
	GPQR	0.1028	0.6508	0.5032	0.0518
	TSVQR	0.1265	0.7867	0.7216	0.0106
0.25	SVQR	0.2220	0.6240	0.4882	0.0904
	ε -SVQR	0.2229	0.6236	0.4874	0.0411
	Online-SVQR	0.4525	1.3422	0.8351	0.0658
	GPQR	0.1518	0.5885	0.3991	0.0496
	TSVQR	0.2323	0.7608	0.6659	0.0091
0.50	SVQR	0.3066	0.7722	0.6133	0.0264
	ε -SVQR	0.3028	0.7646	0.6056	0.0559
	Online-SVQR	0.4695	1.5084	0.9390	0.0412
	GPQR	0.5266	0.8781	0.8332	0.0909
	TSVQR	0.3150	0.7887	0.6300	0.0056
0.75	SVQR	0.4049	0.9126	0.7237	0.0335
	ε -SVQR	0.4029	0.9102	0.7211	0.0450
	Online-SVQR	0.4898	1.7388	1.0769	0.0392
	GPQR	0.4118	0.9419	0.7027	0.0312
	TSVQR	0.3393	0.9015	0.6852	0.0082
0.90	SVQR	0.4669	0.9929	0.7866	0.0265
	ε -SVQR	0.4618	0.9875	0.7810	0.0784
	Online-SVQR	0.5073	1.9096	1.1837	0.0525
	GPQR	0.3586	0.7243	0.7417	0.0294
	TSVQR	0.2943	1.0193	0.7382	0.0065

4.5. The quantile parameter and analysis

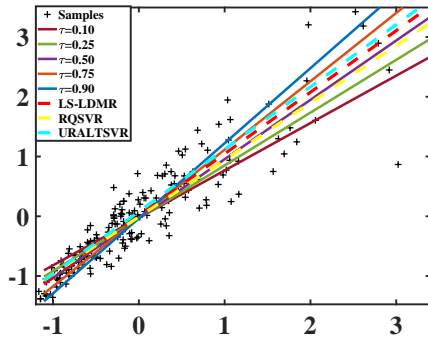
In this part, we adopt immunoglobulin G Data (Isaacs et al., 1983) to analyze the effects of the quantile parameter τ on the regression results. This data set comprises the serum concentration of immunoglobulin G in 298 children aged from 6 months to 6 years. To test the influence of the parameter τ on the Risk, RMSE, MAE, and MAPE, we first fix the parameters C_1 , C_2 , and P as the optimal values selected by the grid search technique. Fig. 12 illustrates the influence of the parameter τ on the regression results. From Fig. 12, we observe that as parameter τ increases, the value of Risk increases and then decreases, which means that parameter τ has a strong influence on the regression results. As τ increases, the value of RMSE decreases and then increases. When $\tau = 0.50$, Risk reaches a maximum value and RMSE reaches



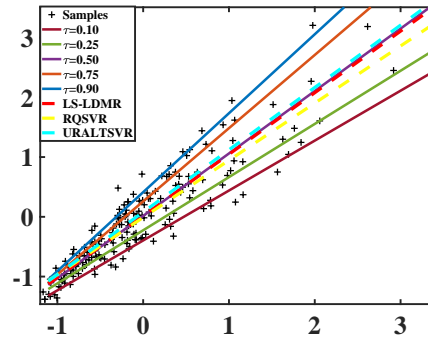
(a) SVQR



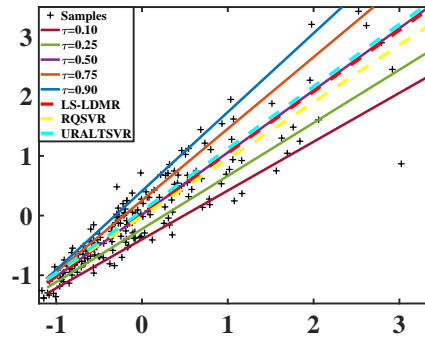
(b) ε -SVQR



(c) Online-SVQR



(d) GPQR



(e) TSVQR

Figure 8: Regression results of SVQR, ε -SVQR, Online-SVQR, GPQR, TSVQR, LS-LDMR, RQSVR, and URALTSVR for Engel data set.

Table 15: Evaluation indices of Bone density data set.

τ	Method	Risk	RMSE	MAE	CPU Time
0.10	SVQR	0.0899	0.1490	0.1369	0.1681
	ε -SVQR	0.1797	0.5471	0.5027	0.1332
	Online-SVQR	0.1152	0.1816	0.1682	0.1506
	GPQR	0.1204	0.8365	0.9482	0.0963
	TSVQR	0.0829	0.8549	0.8293	0.0097
0.25	SVQR	0.1385	0.2510	0.2317	0.1280
	ε -SVQR	0.1504	0.2641	0.2438	0.1401
	Online-SVQR	0.1724	0.2964	0.2718	0.1341
	GPQR	0.2091	0.9018	0.6947	0.0945
	TSVQR	0.1170	0.5639	0.4680	0.0179
0.50	SVQR	0.2039	0.4448	0.4078	0.2035
	ε -SVQR	0.2399	0.5416	0.4797	0.1620
	Online-SVQR	0.2219	0.4920	0.4437	0.1828
	GPQR	0.3116	0.8114	0.6231	0.1066
	TSVQR	0.2138	0.4763	0.4276	0.0134
0.75	SVQR	0.2208	0.5720	0.5233	0.1281
	ε -SVQR	0.2806	0.6786	0.5239	0.1210
	Online-SVQR	0.2199	0.5725	0.5236	0.1245
	GPQR	0.2719	0.7097	0.8073	0.0941
	TSVQR	0.2593	0.9013	0.7808	0.0243
0.90	SVQR	0.1817	0.5445	0.5003	0.1359
	ε -SVQR	0.2640	0.6987	0.6345	0.1161
	Online-SVQR	0.2126	0.6425	0.5924	0.1260
	GPQR	0.1630	0.7442	0.6457	0.0878
	TSVQR	0.1584	1.3002	1.1054	0.0106

a minimum value. From Fig. 12(d), we find that the curve of CPU time fluctuates slightly around approximate value of 0.0115. Fig. 13 demonstrates the effects of parameters C_1 , C_2 , and P on the convergence speed, when $\tau = 0.10, 0.25, 0.50, 0.75$, and 0.90 . From Fig. 13, we find that as parameter τ increases, the convergence speed decreases and then approximately remains the same. As parameters P or C_1 and C_2 increase, all lines in Fig. 13 fluctuate slightly.

Fig. 14 presents the regression results of the lower-bound function $f_1(x)$, the upper-bound function $f_2(x)$, and the final decision function $f(x)$, when $\tau = 0.10, 0.25, 0.50, 0.75$, and 0.90 . As seen from Fig. 14, we see that at each quantile level, $f_1(x)$ depicts the lower-bound distribution information, $f_2(x)$ depicts the upper-bound distribution information, and $f_1(x)$ and $f_2(x)$ are

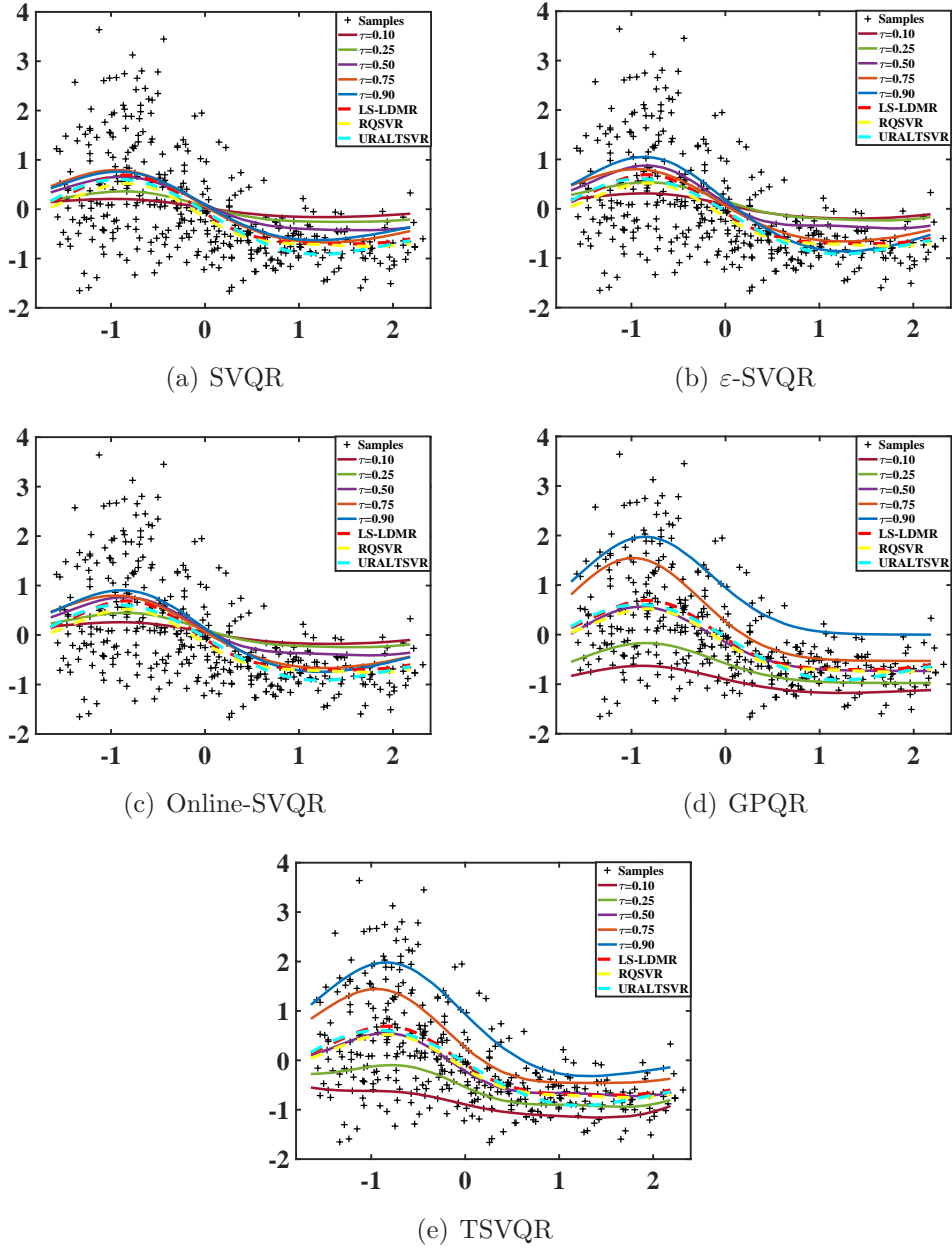


Figure 9: Regression results of SVQR, ε -SVQR, Online-SVQR, GPQR, TSVQR, LS-LDMR, RQSVR, and URALTSVR for Bone density data set.

Table 16: Evaluation indices of US girls data set.

τ	Method	Risk	RMSE	MAE	CPU Time
0.10	SVQR	0.1220	0.9269	0.7635	21.6099
	ε -SVQR	0.1891	0.7500	0.6611	20.4738
	Online-SVQR	0.1513	0.8300	0.7038	21.0418
	GPQR	0.0446	0.6439	0.4128	6.7215
	TSVQR	0.1896	0.7757	0.6762	2.6566
0.25	SVQR	0.3126	0.7758	0.7141	15.9121
	ε -SVQR	0.3573	0.7562	0.6931	14.6243
	Online-SVQR	0.3337	0.7581	0.7011	15.2682
	GPQR	0.6087	0.7303	0.3037	6.2507
	TSVQR	0.3029	0.7958	0.7200	2.2384
0.50	SVQR	0.3989	0.8591	0.7978	14.5569
	ε -SVQR	0.3962	0.8539	0.7923	13.4608
	Online-SVQR	0.3973	0.8556	0.7947	14.0089
	GPQR	0.1261	0.4454	0.2522	6.4887
	TSVQR	0.3948	0.8583	0.7895	1.7579
0.75	SVQR	0.4224	0.9895	0.9126	15.8177
	ε -SVQR	0.4966	0.9864	0.9187	16.7182
	Online-SVQR	0.4576	0.9776	0.9120	16.2679
	GPQR	0.5256	0.4424	0.2512	6.4887
	TSVQR	0.4153	0.9959	0.9100	2.0672
0.90	SVQR	0.5937	1.1482	1.0676	20.6675
	ε -SVQR	0.6405	1.1899	1.1011	20.9365
	Online-SVQR	0.6169	1.1685	1.0839	20.8021
	GPQR	0.0834	0.6751	0.5229	6.1780
	TSVQR	0.3694	1.2542	1.1096	2.5321

nonparallel. $f(x)$ combines the distribution information of $f_1(x)$ and $f_2(x)$, and then presents the information at each quantile location. As the quantile parameter τ ranges from 0.1 to 0.9, we plot the corresponding final decision function $f(x)$ represented by the red solid curves in Fig. 14. Obviously, different quantile locations yield different red solid curves and these curves are nonparallel, indicating that the immunoglobulin G Data reflect potential heterogeneity and asymmetry. Therefore, TSVQR completely captures the heterogeneous and asymmetric information at low and high quantiles of all data points.

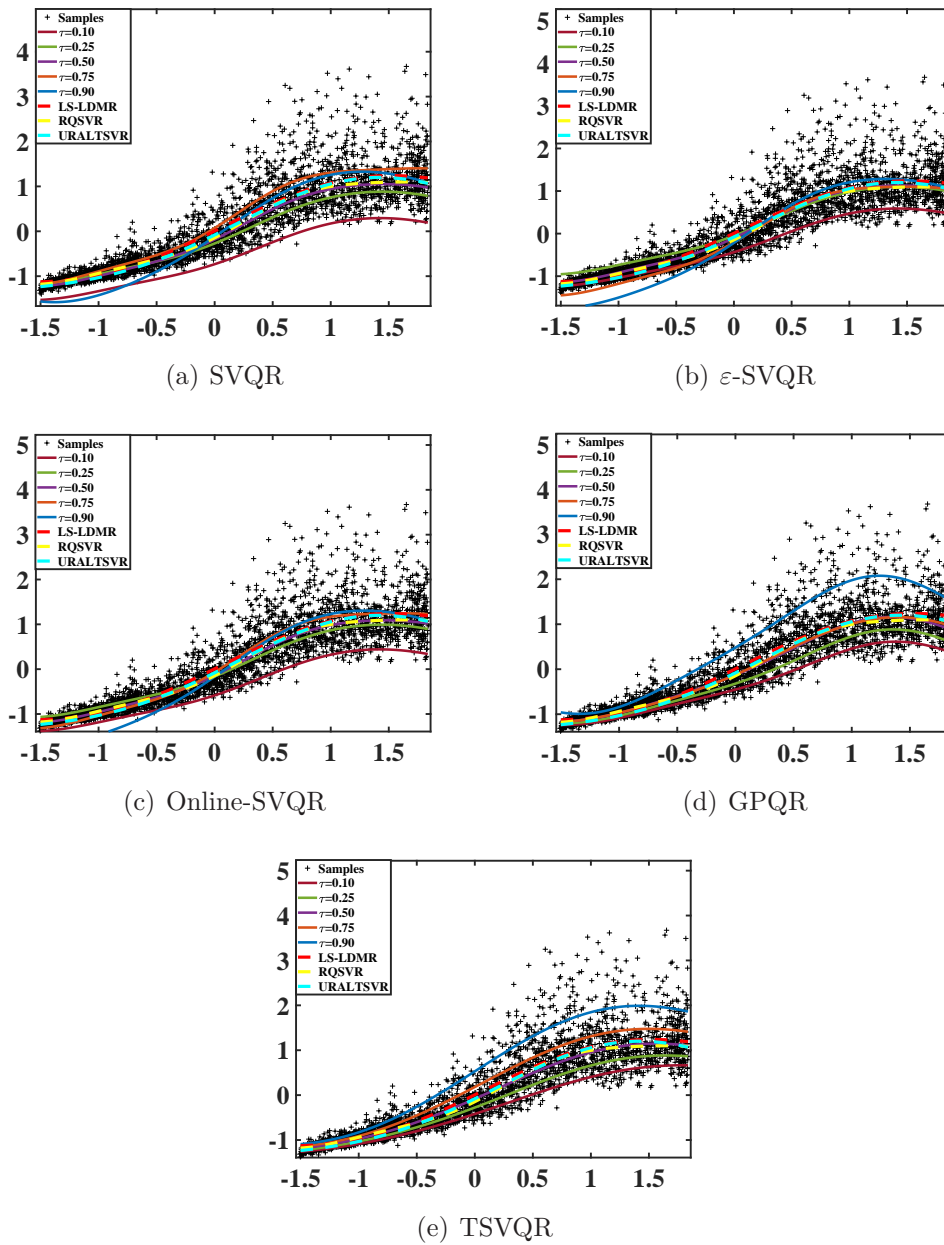


Figure 10: Regression results of SVQR, ε -SVQR, Online-SVQR, GPQR, TSVQR, LS-LDMR, RQSVR, and URALTSVR for US girls data set.

Table 17: Evaluation indices of Motorcycle data set.

τ	Method	Risk	RMSE	MAE	CPU Time
0.10	SVQR	0.3192	0.5218	0.4731	0.0406
	ε -SVQR	0.3090	0.5158	0.4654	0.0312
	Online-SVQR	0.2619	0.7064	0.6194	0.0360
	GPQR	0.1241	0.8311	0.9398	0.0122
	TSVQR	0.1226	0.5645	0.3836	0.0116
0.25	SVQR	0.1856	0.4396	0.3615	0.0303
	ε -SVQR	0.3730	0.6070	0.5606	0.0525
	Online-SVQR	0.2766	0.6789	0.5934	0.0414
	GPQR	0.2546	0.8739	0.7295	0.0112
	TSVQR	0.2266	0.4884	0.4181	0.0088
0.50	SVQR	0.1560	0.4173	0.3119	0.0333
	ε -SVQR	0.1680	0.5027	0.3360	0.0273
	Online-SVQR	0.2375	0.6347	0.4751	0.0303
	GPQR	0.2632	0.6751	0.5263	0.0126
	TSVQR	0.2595	0.6318	0.5191	0.0114
0.75	SVQR	0.3320	0.5514	0.4834	0.0413
	ε -SVQR	0.3287	0.5486	0.4796	0.0305
	Online-SVQR	0.3737	0.6454	0.5315	0.0359
	GPQR	0.2003	0.7043	0.7043	0.0117
	TSVQR	0.1643	0.7127	0.6093	0.0115
0.90	SVQR	0.5958	0.7962	0.7112	0.0287
	ε -SVQR	0.2755	0.4762	0.4222	0.0341
	Online-SVQR	0.5792	0.7512	0.6654	0.0314
	GPQR	0.0997	0.8170	0.9018	0.0188
	TSVQR	0.0784	0.8134	0.7245	0.0130

5. Applications of TSVQR

To validate the regression performance of TSVQR, we provide experiments on several real-world data sets, including large scale data, time series, and imbalanced data.

5.1. Large scale data

Heterogeneity and asymmetry have simultaneously emerged in environment field. We apply TSVQR to predicting the energy use of appliances (Candanedo et al.,2017) and assessing PM2.5 pollution in Beijing (Liang et al., 2015). Appliances energy prediction data set involves 19735 instances and 29 attributes. Beijing PM2.5 data set contains 43824 instances and 13 attributes. We use the first half of each data set for training, and the rest

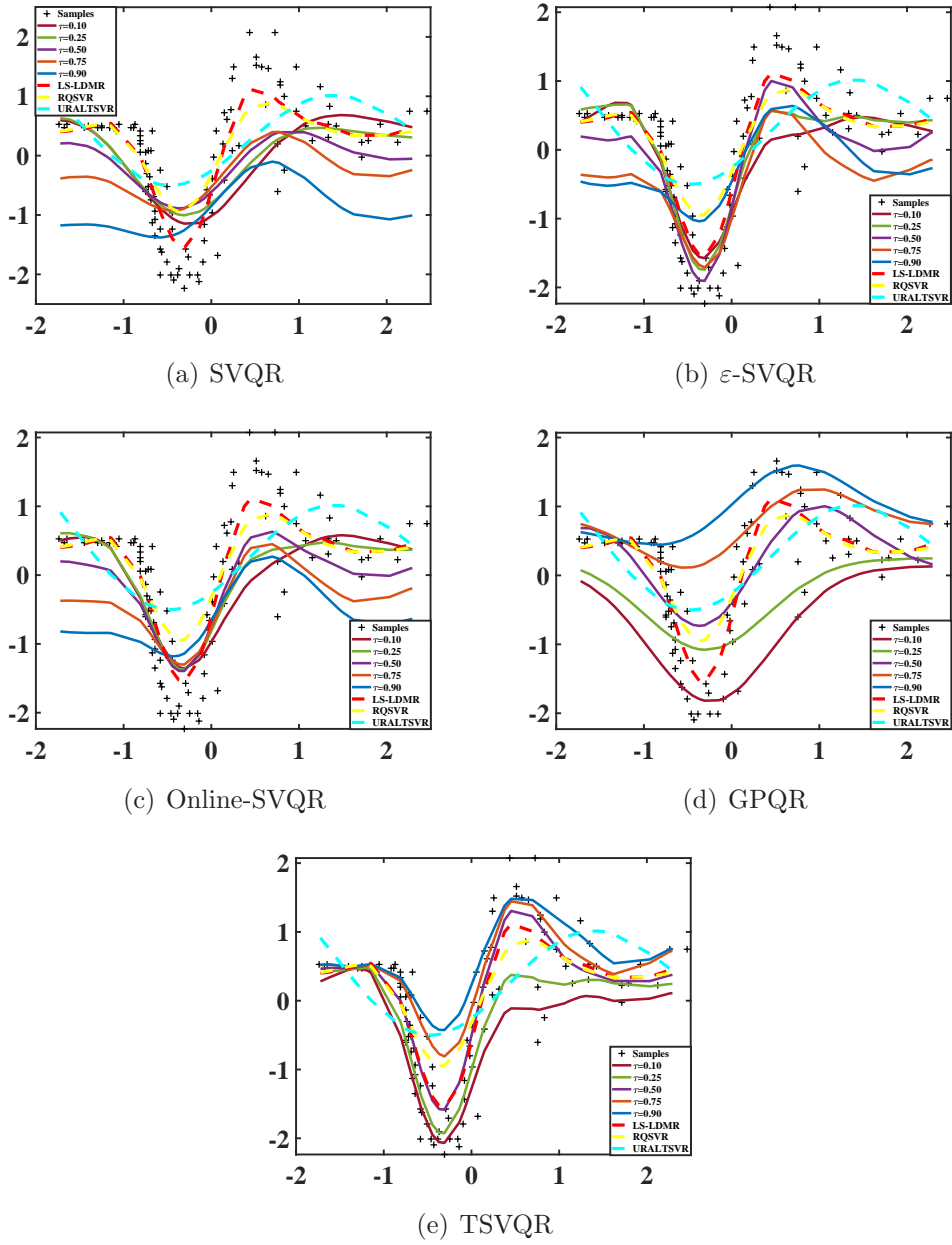
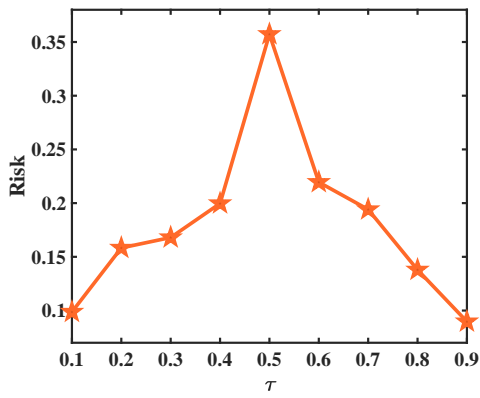
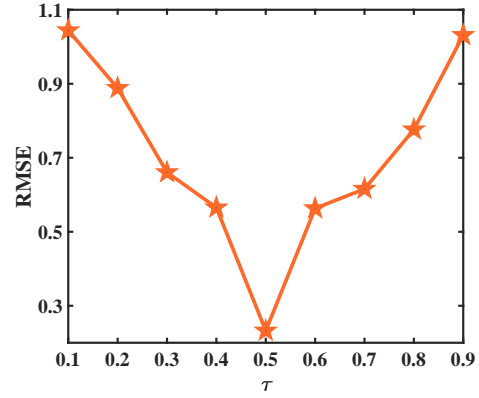


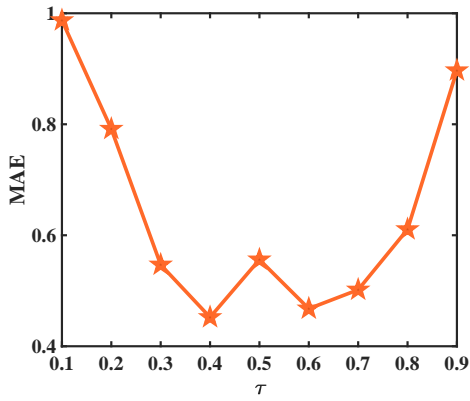
Figure 11: Regression results of SVQR, ε -SVQR, Online-SVQR, GPQR, TSVQR, LS-LDMR, RQSVR, and URALTSVR for Motorcycle data set.



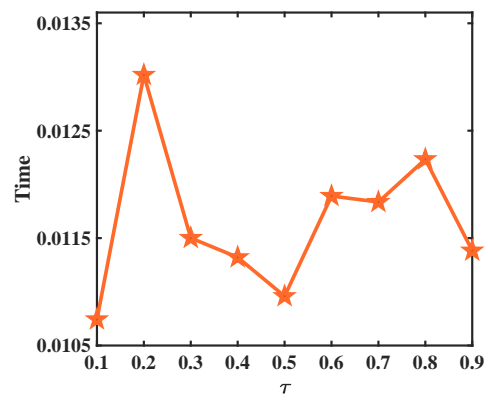
(a) Risk



(b) RMSE

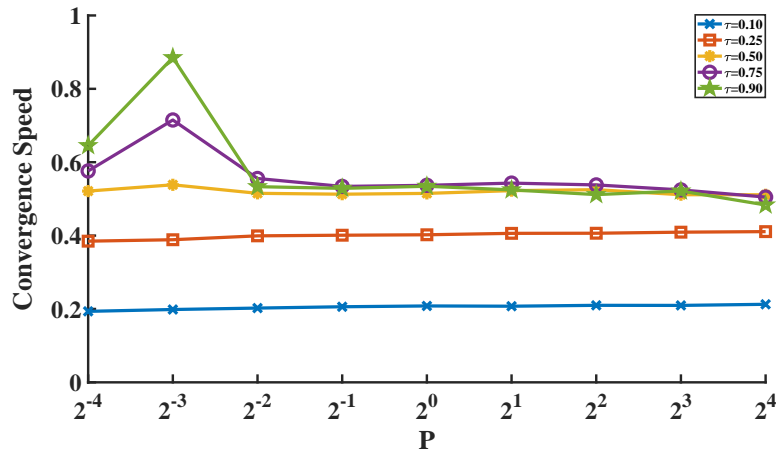


(c) MAE

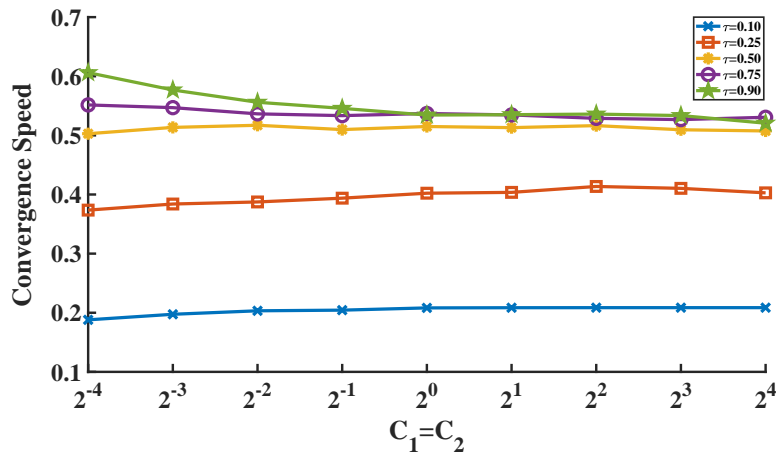


(d) Time

Figure 12: The influence of τ on the Risk, RMSE, MAE, and CPU Time. Parameters C_1 , C_2 , and P are fixed as the optimal values.

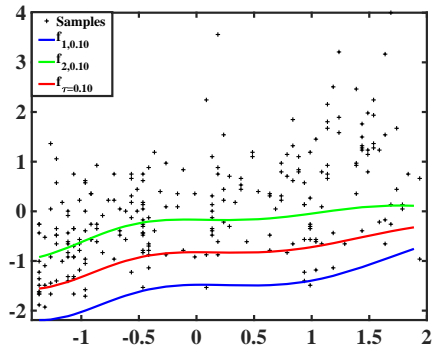


(a)

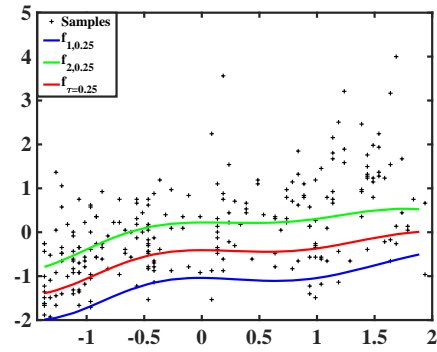


(b)

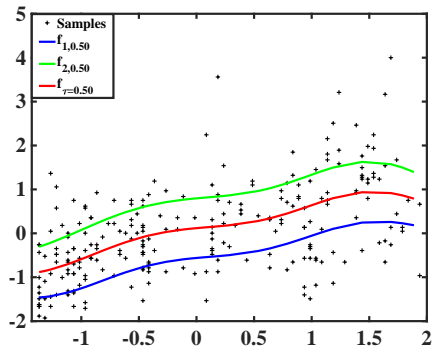
Figure 13: Convergence speed of TSVQR ($\tau = 0.10, 0.25, 0.50, 0.75,$ and 0.90).



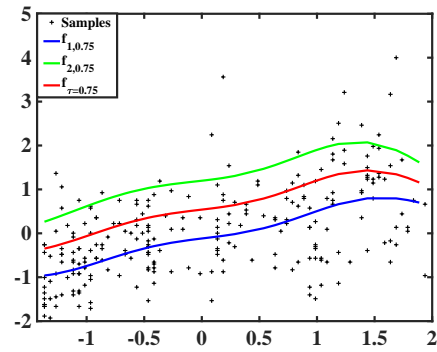
(a) $\tau = 0.10$



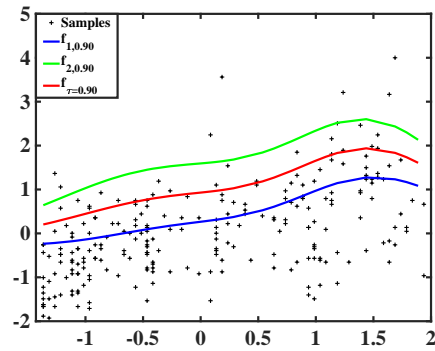
(b) $\tau = 0.25$



(c) $\tau = 0.50$



(d) $\tau = 0.75$



(e) $\tau = 0.90$

Figure 14: Regression results of TSVQR ($\tau = 0.10, 0.25, 0.50, 0.75, \text{ and } 0.90$).

Table 18: Evaluation indices of Boston housing data set.

τ	Method	Risk	RMSE	MAE	CPU Time
0.10	SVQR	0.2112	0.2431	0.2385	0.1543
	ε -SVQR	0.2019	0.2557	0.2439	0.1343
	Online-SVQR	0.2034	0.2437	0.2349	0.1442
	GPQR	0.1827	0.5746	0.4695	0.0610
	TSVQR	0.0183	0.3404	0.1829	0.0398
0.25	SVQR	0.1962	0.2727	0.2678	0.1440
	ε -SVQR	0.1955	0.2997	0.2840	0.1457
	Online-SVQR	0.1926	0.2789	0.2694	0.1449
	GPQR	0.3375	0.6474	0.5164	0.0491
	TSVQR	0.0429	0.3192	0.1711	0.0427
0.50	SVQR	0.0855	0.1745	0.1710	0.1423
	ε -SVQR	0.1053	0.2622	0.2106	0.1313
	Online-SVQR	0.0838	0.1889	0.1676	0.1369
	GPQR	0.3633	0.8783	0.7267	0.0521
	TSVQR	0.0743	0.2851	0.1486	0.0346
0.75	SVQR	0.0367	0.1291	0.1260	0.1471
	ε -SVQR	0.0862	0.2141	0.1388	0.1627
	Online-SVQR	0.0501	0.1351	0.1096	0.1549
	GPQR	0.2233	0.8230	0.8635	0.0684
	TSVQR	0.0641	0.1711	0.0888	0.0210
0.90	SVQR	0.0134	0.1365	0.1331	0.1377
	ε -SVQR	0.0319	0.1419	0.1299	0.1509
	Online-SVQR	0.0172	0.1280	0.1207	0.1443
	GPQR	0.4833	0.9585	0.8493	0.1629
	TSVQR	0.0245	0.0704	0.0392	0.0301

for testing. For the nonlinear TSVQR, we employ a Gaussian kernel, and a wavelet kernel, respectively. All experiments are implemented in the MATLAB R2021a environment on the Ubuntu 20.05 and 128 GB of RAM.

Tables 23 and 24 list the regression results for TSVQR, when $\tau = 0.10$, 0.25, 0.50, 0.75, and 0.90. From both tables, we find that the values of Risk, RMSE, and MAE fluctuate slightly at each quantile level, which means that TSVQR fits the actual data set at every quantile location. Moreover, the regression results of both nonlinear kernel are similar, which is evident that TSVQR effectively captures the heterogeneous and asymmetric information in all data points. As for the training speed, the learning speed of TSVQR fluctuates slightly at each quantile level in Table 24. Therefore, TSVQR receives good regression performance with fast training speed for big data

Table 19: Evaluation indices of Benchmark data sets for LS-LDMR, RQSVR and URALTSVR.

Data set	Method	RMSE	MAE	MAPE	CPU Time
Engel	LS-LDMR	0.7071	0.5671	1.0211	0.0070
	RQSVR	0.5996	0.3412	1.0096	0.0164
	URALTSVR	0.6869	0.3314	1.0428	0.0023
Bone density	LS-LDMR	0.5221	0.4748	1.3127	0.0318
	RQSVR	0.8174	0.6249	2.6513	0.0953
	URALTSVR	0.8185	0.6547	3.0161	0.0147
US girls	LS-LDMR	0.9000	0.8321	0.9710	0.2411
	RQSVR	0.4413	0.2519	0.9336	11.5615
	URALTSVR	0.4386	0.2600	0.8261	2.1039
Motorcycle	LS-LDMR	0.5839	0.5099	1.0010	0.0078
	RQSVR	0.7563	0.5338	1.7136	0.0072
	URALTSVR	0.7743	0.5894	3.8043	0.0117
Boston housing	LS-LDMR	0.2891	0.2519	0.5622	0.0026
	RQSVR	0.9476	0.7607	5.2051	0.0938
	URALTSVR	0.8971	0.6953	3.3802	0.0174

sets.

5.2. Time series

We apply TSVQR to “MelTemp” time series and “Gasprice” time series, which are available in R package. The “MelTemp” data set illustrates daily maximum temperatures in Melbourne, involving 3650 instances. The “Gasprice” data set presents weekly US gasoline price, including 695 instances. We use the forward chaining method to validate the regression performance of TSVQR. Table 25 lists the regression results for TSVQR, when $\tau = 0.10, 0.25, 0.50, 0.75,$ and 0.90 . From Table 25, we find that the values of Risk, RMSE, and MAE fluctuate slightly at each quantile level, which means that TSVQR fits the time series at every quantile location. As for the training speed, the learning speed of TSVQR fluctuates slightly at each quantile level in Table 25.

5.3. Imbalanced data

To validate the asymmetric-information-capturing ability of TSVQR, we consider two imbalanced data sets: “Dermatology” and “Car Evaluation”. The “Dermatology” data set contains 366 instances and 34 attributes. The “Car Evaluation” data set contains 1728 instances and 6 attributes. Both

Table 20: Friedman test of SVQR, ε -SVQR, Online-SVQR, GPQR, and TSVQR.

τ	Evaluation criteria	Value of χ^2	Value of F_F
0.10	Risk	24.1454	12.1612
	CPU Time	27.5636	16.7699
0.25	Risk	17.2363	6.4402
	CPU Time	31.2363	24.4729
0.50	Risk	12.8363	4.1190
	CPU Time	26.8727	15.6900
0.75	Risk	13.3818	4.3705
	CPU Time	23.9273	11.9203
0.90	Risk	21.7454	9.7712
	CPU Time	22.6182	10.5782

Table 21: Nemenyi test of SVQR, ε -SVQR, Online-SVQR, GPQR, and TSVQR.

τ	Comparison	Risk	CPU Time
0.10	TSVQR vs. SVQR	2.0000	3.1818
	TSVQR vs. ε -SVQR	2.3636	1.8181
	TSVQR vs. Online-SVQR	2.2727	2.9090
	TSVQR vs. GPQR	0.1818	2.0909
0.25	TSVQR vs. SVQR	1.7272	2.3636
	TSVQR vs. ε -SVQR	2.2727	2.7272
	TSVQR vs. Online-SVQR	2.5454	2.8181
	TSVQR vs. GPQR	1.6363	2.3636
0.50	TSVQR vs. SVQR	0.9090	2.7272
	TSVQR vs. ε -SVQR	1.7272	2.0000
	TSVQR vs. Online-SVQR	1.4545	2.4545
	TSVQR vs. GPQR	1.9090	2.9090
0.75	TSVQR vs. SVQR	1.8181	2.4545
	TSVQR vs. ε -SVQR	2.0000	2.6363
	TSVQR vs. Online-SVQR	1.8181	2.9090
	TSVQR vs. GPQR	2.0909	2.0000
0.90	TSVQR vs. SVQR	2.2727	2.3636
	TSVQR vs. ε -SVQR	2.2727	2.4545
	TSVQR vs. Online-SVQR	2.4545	2.8181
	TSVQR vs. GPQR	0.7272	2.3636

Table 22: Nemenyi test of SVQR, ε -SVQR, Online-SVQR, GPQR, TSVQR, LS-LDMR, RQSVR and URALTSVR.

Comparison	CPU Time
LS-LDMR vs. SVQR	5.4545
LS-LDMR vs. ε -SVQR	4.2727
LS-LDMR vs. Online-SVQR	5.2727
LS-LDMR vs. GPQR	4.9090
LS-LDMR vs. RQSVR	3.4545
LS-LDMR vs. URALTSVR	1.0909
LS-LDMR vs. TSVQR	1.3636

Table 23: Evaluation indices of appliance energy prediction data set.

τ	0.10	0.25	0.50	0.75	0.90
Gaussian kernel					
Risk	0.2774	0.2880	0.2918	0.2928	0.2921
RMSE	0.9154	0.9551	0.9718	0.9799	0.9943
MAE	0.5711	0.5803	0.5835	0.5847	0.5871
CPU Time	51.8825	52.8494	84.0566	129.2691	142.7396
Wavelet kernel					
Risk	0.2953	0.2952	0.2952	0.2949	0.2948
RMSE	0.9966	0.9967	0.9967	0.9966	0.9967
MAE	0.5901	0.5901	0.5901	0.5901	0.5901
CPU Time	95.4110	59.2504	43.0104	76.8283	75.5245

Table 24: Evaluation indices of Beijing PM2.5 data sets

τ	0.10	0.25	0.50	0.75	0.90
Gaussian kernel					
Risk	0.1545	0.3369	0.5390	0.6605	0.7141
RMSE	1.7663	1.5790	1.3864	1.3976	1.4737
MAE	1.4656	1.3054	1.0780	0.9735	1.0461
CPU Time	779.8702	728.8788	732.0485	728.1161	776.8404
Wavelet kernel					
Risk	0.2179	0.3682	0.5455	0.6655	0.7678
RMSE	1.7392	1.5597	1.4250	1.5307	1.7420
MAE	1.4357	1.2812	1.0910	1.1028	1.3615
CPU Time	755.6335	671.0814	653.9155	653.5467	702.8267

Table 25: Evaluation indices of time series data sets.

τ	0.10	0.25	0.50	0.75	0.90
Gasprice					
Risk	0.0006	0.0013	0.0019	0.0017	0.0008
RMSE	0.0202	0.0248	0.0299	0.0284	0.0226
MAE	0.0026	0.0031	0.0038	0.0036	0.0029
CPU Time	0.0272	0.0232	0.0266	0.0332	0.0256
MelTemp					
Risk	0.0002	0.0003	0.0004	0.0003	0.0001
RMSE	0.0039	0.0089	0.0151	0.0190	0.0202
MAE	0.0002	0.0005	0.0008	0.0010	0.0011
CPU Time	0.9883	0.9836	1.0954	1.0476	0.9943

Table 26: Evaluation indices of Dermatology data sets.

τ	0.10	0.25	0.50	0.75	0.90
Ratio 70% : 30%					
Risk	0.1050	0.1206	0.1198	0.1094	0.0921
RMSE	0.5219	0.3860	0.3470	0.3548	0.4125
MAE	0.3418	0.2649	0.2397	0.2450	0.2937
CPU Time	0.0141	0.0140	0.0139	0.0139	0.0141
Ratio 60% : 40%					
Risk	0.1103	0.1273	0.1261	0.1163	0.0993
RMSE	0.5482	0.4160	0.3649	0.3715	0.4317
MAE	0.3589	0.2823	0.2521	0.2577	0.3101
CPU Time	0.0147	0.0146	0.0147	0.0147	0.0148

data sets, where the total number of samples is not the same in the classes (Gupta et al., 2019), are very popular in the UC Irvine (UCI) Machine Learning Repository. We apply Monte Carlo cross validation (MCCV) with 1000 iterations using the different ratios of 70% : 30% and 60% : 40%. Tables 26 and 27 show the average results of Risk, RMSE, MAE, and CPU time, when $\tau = 0.10, 0.25, 0.50, 0.75,$ and 0.90 . From both data sets, we find that TSVQR gets small Risk at each quantile level, indicating that TSVQR captures the asymmetric information at different quantile location. Moreover, the average training speed of TSVQR fluctuates slightly at different quantile levels. As the number of training samples in the same data set increases, the average training speed decreases.

Table 27: Evaluation indices of Car Evaluation data sets.

τ	0.10	0.25	0.50	0.75	0.90
Ratio 70% : 30%					
Risk	0.0697	0.0924	0.1010	0.0916	0.0768
RMSE	0.6413	0.4679	0.3534	0.3291	0.3510
MAE	0.3027	0.2356	0.2021	0.1966	0.2250
CPU Time	0.1990	0.1982	0.1996	0.1982	0.2130
Ratio 60% : 40%					
Risk	0.0797	0.1031	0.1108	0.1015	0.0871
RMSE	0.6657	0.5035	0.3802	0.3505	0.3715
MAE	0.3247	0.2585	0.2217	0.2155	0.2479
CPU Time	0.1449	0.1432	0.1441	0.1457	0.1547

6. Conclusions

Heterogeneity and asymmetry are two major and common statistical features of modern data. How to capture the heterogeneous and asymmetric information in data is a major challenge for regression technology. This paper proposed a twin support vector quantile regression to efficiently solve this problem. Experimental results on both artificial data sets and real-world data sets demonstrated that TSVQR effectively depicted the heterogeneous and asymmetric information and gave a more complete picture of the data set. The training speed of TSVQR was significantly faster than that of SVQR, ε -SVQR, and Online-SVQR.

Compared with SVQR, ε -SVQR, Online-SVQR, and GPQR, the main strengths of TSVQR are as follows. First, the quantile parameter is adopted in TSVQR to completely measure the heterogeneous information in data points. Second, TSVQR constructed two smaller-sized quadratic programming problems to obtain two nonparallel hyperplanes to depict the asymmetric information at each quantile location. Third, two smaller-sized QPPs made TSVQR work quickly. The dual coordinate descent algorithm to solve the QPPs accelerated the training speed of TSVQR.

Despite several contributions of this study, there are some limitations that should be taken into account in future research. First, how to theoretically determine the optimal parameters of TSVQR for each quantile location is still a question. Second, we construct more reasonable criteria to evaluate the regression results of TSVQR, as some traditional evaluation criteria are only suitable for the conditional mean models. Third, from the application

perspective, how to use the proposed method to deal with the heterogeneous problem or asymmetric problem in the real world remains an open question. For example, heterogeneity and asymmetry have commonly emerged in medicine (Collaboration et al., 2021) and environment (Ahmad & Zhao, 2018; Cheng et al., 2021). The application of TSVQR to both fields especially for big data, time series, or image data is our future work.

Data availability

The code and artificial data that support the findings of this study are available in “<http://www.optimal-group.org/Resources/Code/TSVQR.html>”, the UCI benchmark data that support the findings of this study are available in “<http://archive.ics.uci.edu/ml/index.php>”, and data sets of “Engel”, “Bone density”, “US girls”, “MelTemp”, and “Gasprice” are available in “<https://www.r-project.org>”.

Acknowledgments

This work is supported by the National Natural Science Foundation of China (Nos. 12101552, 11871183, and 61866010), the National Social Science Foundation of China (No. 21BJY256), Philosophy and Social Sciences Leading Talent Training Project of Zhejiang Province (No. 21YJRC07-1YB), the Natural Science Foundation of Zhejiang Province (No. LY21F030013), and the Natural Science Foundation of Hainan Province (No. 120RC449).

References

- Ahmad, M., & Zhao, Z.-Y. (2018). Empirics on linkages among industrialization, urbanization, energy consumption, CO_2 emissions and economic growth: a heterogeneous panel study of china. *Environmental Science and Pollution Research*, *25*, 30617–30632. [10.1007/s11356-018-3054-3](https://doi.org/10.1007/s11356-018-3054-3).
- Anand, P., Rastogi, R., & Chandra, S. (2020). A new asymmetric ε -insensitive pinball loss function based support vector quantile regression model. *Applied Soft Computing*, *94*, 106473. [10.48550/arXiv.1908.06923](https://arxiv.org/abs/1908.06923).
- Bachrach, L. K., Hastie, T., Wang, M.-C., Narasimhan, B., & Marcus, R. (1999). Bone mineral acquisition in healthy asian, hispanic, black, and caucasian youth: a longitudinal study. *The journal of clinical endocrinology & metabolism*, *84*, 4702–4712. [10.1210/jcem.84.12.6182](https://doi.org/10.1210/jcem.84.12.6182).

- Baigh, T. A., Yong, C. C., & Cheong, K. C. (2021). Existence of asymmetry between wages and automatable jobs: a quantile regression approach. *International Journal of Social Economics*, . [10.1108/IJSE-02-2021-0085](https://doi.org/10.1108/IJSE-02-2021-0085).
- Burges, C. J. C. (1998). A tutorial on support vector machines for pattern recognition. *Data Mining and Knowledge Discovery*, *2*, 121–167. [10.1023/A:1009715923555](https://doi.org/10.1023/A:1009715923555).
- Candanedo, L. M., Feldheim, V., & Deramaix, D. (2017). Data driven prediction models of energy use of appliances in a low-energy house. *Energy and buildings*, *140*, 81–97. [10.1016/j.enbuild.2017.01.083](https://doi.org/10.1016/j.enbuild.2017.01.083).
- Cheng, C., Ren, X., Dong, K., Dong, X., & Wang, Z. (2021). How does technological innovation mitigate CO_2 emissions in oecd countries? heterogeneous analysis using panel quantile regression. *Journal of Environmental Management*, *280*, 111818. [10.1016/j.jenvman.2020.111818](https://doi.org/10.1016/j.jenvman.2020.111818).
- Cole, T. J. (1988). Fitting smoothed centile curves to reference data. *Journal of the Royal Statistical Society: Series A (Statistics in Society)*, *151*, 385–406. [10.2307/2982992](https://doi.org/10.2307/2982992).
- Collaboration, N. R. F. et al. (2021). Heterogeneous contributions of change in population distribution of body mass index to change in obesity and underweight. *Elife*, *10*, e60060. [10.7554/eLife.60060](https://doi.org/10.7554/eLife.60060).
- Dempster, A. P., Schatzoff, M., & Wermuth, N. (1977). A simulation study of alternatives to ordinary least squares. *Journal of the American Statistical Association*, *72*, 77–91. [10.2307/2286909](https://doi.org/10.2307/2286909).
- Demšar, J. (2006). Statistical comparisons of classifiers over multiple data sets. *The Journal of Machine learning research*, *7*, 1–30. [10.1162/089976699300016007](https://doi.org/10.1162/089976699300016007).
- Dirick, L., Claeskens, G., Vasnev, A., & Baesens, B. (2021). A hierarchical mixture cure model with unobserved heterogeneity for credit risk. *Econometrics and Statistics*, . [10.1016/j.ecosta.2020.12.002](https://doi.org/10.1016/j.ecosta.2020.12.002).
- Drucker, H., Burges, C. J., Kaufman, L., Smola, A. J., & Vapnik, V. (1997). Support vector regression machines. In *Advances in Neural Information Processing Systems* (pp. 155–161).

- Gu, B., Cao, J., Pan, F., & Xiong, W. (2023). Incremental learning for lagrangian ε -twin support vector regression. *Soft Computing*, (pp. 1–19). [10.1007/s00500-022-07755-9](https://doi.org/10.1007/s00500-022-07755-9).
- Gupta, D., & Gupta, U. (2021a). On robust asymmetric lagrangian ν -twin support vector regression using pinball loss function. *Applied Soft Computing*, *102*, 107099. [10.1016/j.asoc.2021.107099](https://doi.org/10.1016/j.asoc.2021.107099).
- Gupta, D., Richhariya, B., & Borah, P. (2019). A fuzzy twin support vector machine based on information entropy for class imbalance learning. *Neural Computing and Applications*, *31*, 7153–7164. [10.1007/s00521-018-3551-9](https://doi.org/10.1007/s00521-018-3551-9).
- Gupta, U., & Gupta, D. (2019). An improved regularization based lagrangian asymmetric ν -twin support vector regression using pinball loss function. *Applied Intelligence*, *49*, 3606–3627. [10.1007/s10489-019-01465-w](https://doi.org/10.1007/s10489-019-01465-w).
- Gupta, U., & Gupta, D. (2021b). Least squares large margin distribution machine for regression. *Applied Intelligence*, *51*, 7058–7093. [10.1007/s10489-020-02166-5](https://doi.org/10.1007/s10489-020-02166-5).
- Gupta, U., & Gupta, D. (2021c). On regularization based twin support vector regression with huber loss. *Neural Processing Letters*, *53*, 459–515. [10.1007/s11063-020-10380-y](https://doi.org/10.1007/s11063-020-10380-y).
- Härdle, W. (1990). *Applied nonparametric regression*. Cambridge university press.
- Harrison Jr, D., & Rubinfeld, D. L. (1978). Hedonic housing prices and the demand for clean air. *Journal of environmental economics and management*, *5*, 81–102. [10.1016/0095-0696\(78\)90006-2](https://doi.org/10.1016/0095-0696(78)90006-2).
- Higgins, J. P., & Thompson, S. G. (2002). Quantifying heterogeneity in a meta-analysis. *Statistics in medicine*, *21*, 1539–1558. [10.1002/sim.1186](https://doi.org/10.1002/sim.1186).
- Hsieh, C.-J., Chang, K.-W., Lin, C.-J., Keerthi, S. S., & Sundararajan, S. (2008). A dual coordinate descent method for large-scale linear svm. In *Proceedings of the 25th international conference on Machine learning* (pp. 408–415). [10.1145/1390156.1390208](https://doi.org/10.1145/1390156.1390208).
- Irfan, M., Razzaq, A., Suksatan, W., Sharif, A., Elavarasan, R. M., Yang, C., Hao, Y., & Rauf, A. (2022). Asymmetric impact of

- temperature on covid-19 spread in india: Evidence from quantile-on-quantile regression approach. *Journal of Thermal Biology*, *104*, 103101. [10.1016/j.jtherbio.2021.103101](https://doi.org/10.1016/j.jtherbio.2021.103101).
- Isaacs, D., Altman, D., Tidmarsh, C., Valman, H., & Webster, A. (1983). Serum immunoglobulin concentrations in preschool children measured by laser nephelometry: reference ranges for igg, iga, igm. *Journal of clinical pathology*, *36*, 1193–1196. [10.1136/jcp.36.10.1193](https://doi.org/10.1136/jcp.36.10.1193).
- Khan, Y. A., Fan, E., & Ferguson, N. D. (2021). Precision medicine and heterogeneity of treatment effect in therapies for ards. *Chest*, *160*, 1729–1738. [10.1016/j.chest.2021.07.009](https://doi.org/10.1016/j.chest.2021.07.009).
- Koenker, R. (2005). Quantile regression, . [10.1017/CBO9780511754098](https://doi.org/10.1017/CBO9780511754098).
- Koenker, R., & Bassett, G. (1978). Regression quantiles. *Econometrica: journal of the Econometric Society*, (pp. 33–50). [10.2307/1913643](https://doi.org/10.2307/1913643).
- Koenker, R., & Bassett Jr, G. (1982). Robust tests for heteroscedasticity based on regression quantiles. *Econometrica: Journal of the Econometric Society*, (pp. 43–61). [10.2307/1912528](https://doi.org/10.2307/1912528).
- Kolasa, M. (2009). Structural heterogeneity or asymmetric shocks? poland and the euro area through the lens of a two-country dsge model. *Economic Modelling*, *26*, 1245–1269. [10.1016/j.econmod.2009.06.001](https://doi.org/10.1016/j.econmod.2009.06.001).
- Kundaje, A., Kyriazopoulou-Panagiotopoulou, S., Libbrecht, M., Smith, C. L., Raha, D., Winters, E. E., Johnson, S. M., Snyder, M., Batzoglou, S., & Sidow, A. (2012). Ubiquitous heterogeneity and asymmetry of the chromatin environment at regulatory elements. *Genome research*, *22*, 1735–1747. [10.1101/gr.136366.111](https://doi.org/10.1101/gr.136366.111).
- Li, Y., Liu, Y., & Zhu, J. (2007). Quantile regression in reproducing kernel hilbert spaces. *Journal of the American Statistical Association*, *102*, 255–268. [10.1198/016214506000000979](https://doi.org/10.1198/016214506000000979).
- Liang, X., Zou, T., Guo, B., Li, S., Zhang, H., Zhang, S., Huang, H., & Chen, S. X. (2015). Assessing Beijing’s pm2.5 pollution: severity, weather impact, apec and winter heating. *Proceedings of the Royal Society A: Mathematical, Physical and Engineering Sciences*, *471*, 20150257. [10.1098/rspa.2015.0257](https://doi.org/10.1098/rspa.2015.0257).

- Miller, B. F., Bambah-Mukku, D., Dulac, C., Zhuang, X., & Fan, J. (2021). Characterizing spatial gene expression heterogeneity in spatially resolved single-cell transcriptomic data with nonuniform cellular densities. *Genome research*, *31*, 1843–1855. [10.1101/gr.271288.120](https://doi.org/10.1101/gr.271288.120).
- Ouhourane, M., Yang, Y., Benedet, A. L., & Oualkacha, K. (2022). Group penalized quantile regression. *Statistical Methods & Applications*, *31*, 495–529. [10.1007/s10260-021-00580-8](https://doi.org/10.1007/s10260-021-00580-8).
- Park, J., & Kim, J. (2011). Quantile regression with an ε -insensitive loss in a reproducing kernel hilbert space. *Statistics & probability letters*, *81*, 62–70. [10.1016/j.spl.2010.09.019](https://doi.org/10.1016/j.spl.2010.09.019).
- Peng, X. (2010). Tsvr: an efficient twin support vector machine for regression. *Neural Networks*, *23*, 365–372. [10.1016/j.neunet.2009.07.002](https://doi.org/10.1016/j.neunet.2009.07.002).
- Schölkopf, B., Smola, A. J., Williamson, R. C., & Bartlett, P. L. (2000). New support vector algorithms. *Neural computation*, *12*, 1207–1245. [10.1162/089976600300015565](https://doi.org/10.1162/089976600300015565).
- Shao, Y., Zhang, C., Yang, Z., Jing, L., & Deng, N. (2013). An ε -twin support vector machine for regression. *Neural Computing and Applications*, *23*, 175–185. [10.1007/s00521-012-0924-3](https://doi.org/10.1007/s00521-012-0924-3).
- Shi, T., & Chen, S. (2023). Robust twin support vector regression with smooth truncated h ε loss function. *Neural Processing Letters*, (pp. 1–45). [10.1007/s11063-023-11198-0](https://doi.org/10.1007/s11063-023-11198-0).
- Takeuchi, I., Le, Q. V., Sears, T. D., & Smola, A. J. (2006). Nonparametric quantile estimation. *Journal of Machine Learning Research*, *7*, 1231–1264. [10.1007/s10846-006-9065-1](https://doi.org/10.1007/s10846-006-9065-1).
- Tran, T. Q., Pham, H. H., Vo, H. T., Luu, H. T., & Nguyen, H. M. (2019). Local governance, education and occupation-education mismatch: Heterogeneous effects on wages in a lower middle income economy. *International Journal of Educational Development*, *71*, 102101. [10.1016/j.ijedudev.2019.102101](https://doi.org/10.1016/j.ijedudev.2019.102101).
- Wang, L. (2017). Heterogeneous data and big data analytics. *Automatic Control and Information Sciences*, *3*, 8–15. [10.12691/acis-3-1-3](https://doi.org/10.12691/acis-3-1-3).

- Wang, S., Shin, M., & Bai, R. (2023a). Generative quantile regression with variability penalty. *arXiv preprint arXiv:2301.03661*, . [10.48550/arXiv.2301.03661](https://doi.org/10.48550/arXiv.2301.03661).
- Wang, Y.-G., Wu, J., Hu, Z.-H., & McLachlan, G. J. (2023b). A new algorithm for support vector regression with automatic selection of hyperparameters. *Pattern Recognition*, *133*, 108989. [10.1016/j.patcog.2022.108989](https://doi.org/10.1016/j.patcog.2022.108989).
- Wu, J., & Wang, Y. (2022). Iterative learning in support vector regression with heterogeneous variances. *IEEE Transactions on Emerging Topics in Computational Intelligence*, . [10.1109/TETCI.2022.3182725](https://doi.org/10.1109/TETCI.2022.3182725).
- Xu, Q., Zhang, J., Jiang, C., Huang, X., & He, Y. (2015). Weighted quantile regression via support vector machine. *Expert Systems with Applications*, *42*, 5441–5451. [10.1016/j.eswa.2015.03.003](https://doi.org/10.1016/j.eswa.2015.03.003).
- Xu, Y., Li, X., Pan, X., & Yang, Z. (2018). Asymmetric ν -twin support vector regression. *Neural Computing and Applications*, *30*, 3799–3814. [10.1007/s00521-017-2966-z](https://doi.org/10.1007/s00521-017-2966-z).
- Yang, L., & Dong, H. (2019). Robust support vector machine with generalized quantile loss for classification and regression. *Applied Soft Computing*, *81*, 105483. [10.1016/j.asoc.2019.105483](https://doi.org/10.1016/j.asoc.2019.105483).
- Yang, X., Wu, H., Ren, S., Ran, Q., & Zhang, J. (2021). Does the development of the internet contribute to air pollution control in china? mechanism discussion and empirical test. *Structural Change and Economic Dynamics*, *56*, 207–224. [10.1016/j.strueco.2020.12.001](https://doi.org/10.1016/j.strueco.2020.12.001).
- Ye, Y., Chen, S., & Li, C. (2022). Financial technology as a driver of poverty alleviation in china: Evidence from an innovative regression approach. *Journal of Innovation & Knowledge*, *7*, 100164. [10.1016/j.jik.2022.100164](https://doi.org/10.1016/j.jik.2022.100164).
- Ye, Y., Gao, J., Shao, Y., Li, C., Jin, Y., & Hua, X. (2020). Robust support vector regression with generic quadratic nonconvex ε -insensitive loss. *Applied Mathematical Modelling*, *82*, 235–251. [10.1016/j.apm.2020.01.053](https://doi.org/10.1016/j.apm.2020.01.053).
- Ye, Y., Shao, Y., Li, C., Hua, X., & Guo, Y. (2021). Online support vector quantile regression for the dynamic time series with heavy-tailed noise. *Applied Soft Computing*, *110*, 107560. [10.1016/j.asoc.2021.107560](https://doi.org/10.1016/j.asoc.2021.107560).

Yuan, M. (2006). Gacv for quantile smoothing splines. *Computational statistics & data analysis*, 50, 813–829. [10.1016/j.csda.2004.10.008](https://doi.org/10.1016/j.csda.2004.10.008).